THE EUROPEAN
PHYSICAL JOURNAL C

$b \to c\tau\nu$ transitions in the standard model effective field theory

Quan-Yi Hu[a]**, Xin-Qiang Li**[b]**, Ya-Dong Yang**[c]

Key Laboratory of Quark and Lepton Physics (MOE), Institute of Particle Physics, Central China Normal University, Wuhan 430079, Hubei, China

Abstract The $R(D^{(*)})$ anomalies observed in $B \to D^{(*)}\tau\nu$ decays have attracted much attention in recent years. In this paper, we study the $B \to D^{(*)}\tau\nu$, $\Lambda_b \to \Lambda_c\tau\nu$, $B_c \to (J/\psi, \eta_c)\tau\nu$, $B \to X_c\tau\nu$, and $B_c \to \tau\nu$ decays, all being mediated by the same quark-level $b \to c\tau\nu$ transition, in the Standard Model Effective Field Theory. The most relevant dimension-six operators for these processes are $Q_{lq}^{(3)}$, Q_{ledq}, $Q_{lequ}^{(1)}$, and $Q_{lequ}^{(3)}$ in the Warsaw basis. Evolution of the corresponding Wilson coefficients from the new physics scale $\Lambda = 1$ TeV down to the characteristic scale $\mu_b \simeq m_b$ is performed at three-loop in QCD and one-loop in EW/QED. It is found that, after taking into account the constraint $\mathcal{B}(B_c \to \tau\nu) \lesssim 10\%$, a single $\left[C_{lq}^{(3)}\right]_{3323}(\Lambda)$ or $\left[C_{lequ}^{(3)}\right]_{3332}(\Lambda)$ can still be used to resolve the $R(D^{(*)})$ anomalies at 1σ, while a single $\left[C_{lequ}^{(1)}\right]_{3332}(\Lambda)$ is already ruled out by the measured $R(D^{(*)})$ at more than 3σ. By minimizing the $\chi^2(C_i)$ function constructed based on the current data on $R(D)$, $R(D^*)$, $P_\tau(D^*)$, $R(J/\psi)$, and $R(X_c)$, we obtain eleven most trustworthy scenarios, each of which can provide a good explanation of the $R(D^{(*)})$ anomalies at 1σ. To further discriminate these different scenarios, we predict thirty-one observables associated with the processes considered under each NP scenario. It is found that most of the scenarios can be differentiated from each other by using these observables and their correlations.

1 Introduction

In the past few years, the B-physics experiments have reported a number of interesting anomalies in the semi-leptonic B-meson decays, which have aroused a lot of attention [1–3]. In the charged-current processes $B \to D^{(*)}\ell\nu$,

for example, the ratios of the branching fractions[1]

$$R(D^{(*)}) = \frac{\mathcal{B}(B \to D^{(*)}\tau\nu)}{\mathcal{B}(B \to D^{(*)}\ell\nu)}, \tag{1.1}$$

have been measured by the BaBar [4,5] and Belle [6–9] collaborations with $\ell = e, \mu$, as well as the LHCb [10–12] experiment with $\ell = \mu$. These measurements have been averaged by the Heavy Flavor Averaging Group (HFLAV) [13], and the latest results read [14]

$$R(D)^{\text{avg}} = 0.407 \pm 0.039 \pm 0.024,$$
$$R(D^*)^{\text{avg}} = 0.306 \pm 0.013 \pm 0.007, \tag{1.2}$$

with a correlation of -0.203. Comparing Eq. (1.2) with the arithmetic average [14] of the latest Standard Model (SM) predictions [15–18],

$$R(D) = 0.299 \pm 0.003, \quad R(D^*) = 0.258 \pm 0.005, \tag{1.3}$$

one can see that the difference between experiment and theory is at about 3.78σ corresponding to 99.98% confidence level (C.L.), implying therefore intriguing hints of lepton-flavour universality violating new physics (NP) beyond the SM. To understand these anomalies, many studies have been done; see for instance Ref. [19] and references therein, as well as Refs. [20–54].

On the other hand, in view of the absence (so far) of any clear signal of new particles at the LHC, the NP scale Λ should be much higher than the electroweak (EW) scale $\mu_{\text{EW}} \simeq 246$ GeV. Assuming further that there exist no undiscovered but weakly coupled light particles, any NP effect in the processes proceeding at energy scales well below Λ but above μ_{EW} can be effectively described by a series of higher dimensional operators that are built out of the SM fields and are invariant under the SM gauge group

[a] e-mail: qyhu@mails.ccnu.edu.cn

[b] e-mail: xqli@mail.ccnu.edu.cn

[c] e-mail: yangyd@mail.ccnu.edu.cn

---

[1] The advantage of considering the ratios $R(D^{(*)})$ instead of the branching fractions themselves lies in the fact that, apart from the significant reduction of the experimental systematic uncertainties, the CKM matrix element V_{cb} cancels out and the sensitivity to the $B \to D^{(*)}$ transition form factors becomes much weaker.

$SU(3)_C \otimes SU(2)_L \otimes U(1)_Y$ [55,56]. The resulting effective field theory (EFT) is conventionally called the Standard Model Effective Field Theory (SMEFT) [57–59], which has now emerged as one of the most interesting tools to probe systematically the data from the LHC and elsewhere for possible NP hints.[2] For energies below Λ, the leading NP contributions in the SMEFT formalism arise from the dimension-six operators,[3] which were firstly classified in Ref. [55], but found to be redundant for some of them. The first complete and non-redundant basis of dimension-six operators was derived in Ref. [56] and is now commonly called the Warsaw basis.[4] The complete one-loop anomalous dimensions of these dimension-six operators have also been calculated in Refs. [70–72].

The EFT approach is also an essential ingredient for B-physics analyses both within and beyond the SM. As the typical energy scale μ_b is around the bottom-quark mass $m_b \simeq 5$ GeV, being much smaller than the EW and the NP scale, all the B-physics processes can be well described by an effective Lagrangian constructed by integrating out the SM and NP heavy degrees of freedom (for classical reviews, see for example Refs. [73,74]). The resulting EFT includes only the QCD and QED gauge interactions coupled to all the six leptons and the five lightest quarks, plus a full set of dimension-six local operators built with these matter fields as well as the gluon and photon field-strength tensors, and is conventionally called the weak effective theory (WET) [75–77]. In contrast to the SMEFT case, the dimension-six operators in WET are not invariant under the full SM gauge group, but only under $SU(3)_C \otimes U(1)_{em}$, as this EFT is defined below the EW scale where $SU(2)_L \otimes U(1)_Y$ is already broken. A complete and non-redundant set of dimension-six operators relevant for B physics, together with the complete one-loop anomalous dimensions in QCD and QED, can be found in Refs. [75–77].

For a given set of SMEFT dimension-six operators with the corresponding Wilson coefficients specified at the scale Λ, to study their effects on the B-physics processes, one has to follow the following three steps [78]: perform the renormalization group evolution (RGE) of the SMEFT Wilson coefficients from the NP down to the EW scale [70–72]; match the given set of SMEFT operators onto the WET ones at the EW scale [76,79]; perform the RGE of the WET Wilson coefficients from the EW down to the scale μ_b [75–77].

With the aid of these three steps, one can then bridge the gap between the SMEFT Lagrangian and the low-energy measurements in B physics. In this paper, following this procedure and motivated by the $R(D^{(*)})$ anomalies, we shall study the $B \to D^{(*)}\tau\nu$, $\Lambda_b \to \Lambda_c\tau\nu$, $B_c \to (J/\psi, \eta_c)\tau\nu$, $B \to X_c\tau\nu$, as well as $B_c \to \tau\nu$ decays, all being mediated by the same quark-level $b \to c\tau\nu$ transition, in the SMEFT formalism. It is found that the most relevant operators for these processes are $Q_{lq}^{(3)}$, Q_{ledq}, $Q_{lequ}^{(1)}$, and $Q_{lequ}^{(3)}$ in the Warsaw basis. The RGEs of the corresponding Wilson coefficients from the NP scale Λ down to the typical scale μ_b is performed at three-loop in QCD and one-loop in EW/QED (see Refs. [80–82] and references therein). Confronted with the currently available data, we shall also perform a detailed phenomenological analysis of these decays.

Our paper is organized as follows. In Sect. 2, after recapitulating the SMEFT Lagrangian, we list the most relevant dimension-six operators for $b \to c\tau\nu$ transitions, and then discuss the evolution and matching of these operators in both the SMEFT and WET. In Sect. 3, all the observables considered in the paper are listed, and the corresponding inputs for the transition form factors are also mentioned. Our numerical results and discussions are presented in Sect. 4. Finally, we make our conclusions in Sect. 5. Explicit expressions of the helicity amplitudes for $\Lambda_b \to \Lambda_c\tau\nu$ decay are collected in the "Appendix".

2 Theoretical framework

2.1 SMEFT Lagrangian

Following the common practice to truncate the SMEFT Lagrangian at dimension-six level and assuming that the EW symmetry breaking is realized linearly, we can write the SMEFT Lagrangian as

$$\mathcal{L}_{SMEFT} = \mathcal{L}_{SM}^{(4)} + \frac{1}{\Lambda^2}\sum_i C_i(\Lambda)Q_i, \qquad (2.1)$$

where $\mathcal{L}_{SM}^{(4)}$ is the usual SM Lagrangian before spontaneous symmetry breaking (SSB). The dimension-six operators Q_i, which are obtained by integrating out all the heavy NP particles and are invariant under the SM gauge symmetry, are given by

$$Q_{lq}^{(3)} = (\bar{l}\gamma_\mu\tau^I l)(\bar{q}\gamma^\mu\tau^I q), \quad Q_{ledq} = (\bar{l}^j e)(\bar{d}q^j),$$
$$Q_{lequ}^{(1)} = (\bar{l}^j e)\varepsilon_{jk}(\bar{q}^k u), \qquad Q_{lequ}^{(3)} = (\bar{l}^j\sigma_{\mu\nu}e)\varepsilon_{jk}(\bar{q}^k\sigma^{\mu\nu}u),$$
$$(2.2)$$

and so on [55,56]. Here τ^I are the Pauli matrices, and ε_{jk} is the totally antisymmetric tensor with $\varepsilon_{12} = +1$. The fields q and l correspond to the quark and lepton $SU(2)_L$ doublets,

---

[2] See, for example, Refs. [60–63] for recent reviews on the SMEFT.

[3] There exists only a single dimension-five operator in the SMEFT, up to Hermitian conjugation and flavour assignments [56,64]. It violates the lepton number and, after the EW symmetry breaking, gives Majorana masses for the SM neutrinos. This operator is irrelevant to this paper.

[4] Apart from the Warsaw basis [56], other bases were also proposed, with the most prominent ones being the HISZ [65] and the SILH [66,67] basis. For an easy translation between these different bases, one can resort to the computer codes Rosetta [68] and WCxf [69].

while u, d and e are the right-handed $SU(2)_L$ singlets. All the NP contributions are encoded in the Wilson coefficients C_i, which are dependent on the renormalization scale. This scale dependence will, however, be canceled in a physical amplitude by that of the matrix elements of Q_i.

In this paper, we focus only on the operators $Q_{lq}^{(3)}$, Q_{ledq}, $Q_{lequ}^{(1)}$ and $Q_{lequ}^{(3)}$, as well as their hermitian conjugates, which contribute to the $b \rightarrow c\tau\nu$ transitions at tree level [79,82]. Note that the operator $Q_{lq}^{(3)}$ is already self-conjugate [55, 56]. We also assume that the flavour of the neutrino in these operators is pure ν_τ.

2.2 Evolution and matching

To explore the NP effect on the $b \rightarrow c\tau\nu$ transitions, we should firstly link the SMEFT Lagrangian given at the NP scale Λ to the WET Lagrangian given at the typical energy scale μ_b associated with the processes considered. This can be achieved through the following three steps, details of which could be found, for example, in Refs. [75–79].

Firstly, we should evolve the Wilson coefficients C_i of the SMEFT Lagrangian from the initial scale Λ down to the EW scale μ_{EW}, under the SM gauge group $SU(3)_C \otimes SU(2)_L \otimes U(1)_Y$. For simplicity, here we do not discriminate the masses of $W^\pm$, Z^0, the top quark t, and the Higgs boson h, and set approximately all of them to be μ_{EW}. The one-loop RGE flow of $C_i(\mu)$ can be written schematically as

$$\mu \frac{\mathrm{d}C_i}{\mathrm{d}\mu} = \frac{1}{16\pi^2} \sum_j \gamma_{ij} C_j \equiv \frac{1}{16\pi^2} \beta_i. \tag{2.3}$$

Neglecting terms suppressed by the Yukawa couplings, which are found to be negligibly small in our case, the one-loop beta functions are given, respectively, by [70–72,83]

$$\left[\beta_{lq}^{(3)}\right]_{prst} = \frac{2}{3}g^2 \left\{3\left[C_{lq}^{(3)}\right]_{prww}\delta_{st} + \left[C_{lq}^{(3)}\right]_{wwst}\delta_{pr}\right\}$$
$$- (6g^2 + g'^2)\left[C_{lq}^{(3)}\right]_{prst}, \tag{2.4}$$

$$\beta_{ledq} = -\left(\frac{8}{3}g'^2 + 8g_s^2\right)C_{ledq}, \tag{2.5}$$

$$\beta_{lequ}^{(1)} = -\left(\frac{11}{3}g'^2 + 8g_s^2\right)C_{lequ}^{(1)}$$
$$+ \left(30g'^2 + 18g^2\right)C_{lequ}^{(3)}, \tag{2.6}$$

$$\beta_{lequ}^{(3)} = \left(\frac{2}{9}g'^2 - 3g^2 + \frac{8}{3}g_s^2\right)$$
$$\times C_{lequ}^{(3)} + \frac{1}{8}(5g'^2 + 3g^2)C_{lequ}^{(1)}. \tag{2.7}$$

Here we have introduced the abbreviations $\left[C_{lq}^{(3)}\right]_{.ww.} \equiv \sum_w \left[C_{lq}^{(3)}\right]_{.ww.}$, with p, r, s, t, w being the flavour indices

of the fermion fields in the weak-eigenstate basis, and g_s, g and g' are the $SU(3)_C$, $SU(2)_L$ and $U(1)_Y$ gauge couplings, respectively. The SMEFT Lagrangian will undergo the SSB at an energy scale close to μ_{EW}, making it necessary to switch from the weak to the mass eigenstates for the fermions. Performing the same flavour transformations as in Refs. [76,77,79,84], we can write the spontaneously broken SMEFT Lagrangian in terms of the mass-eigenstate fermion fields ($f_{L,R}^{(\text{weak})} = P_{L,R}f^{(\text{mass})}$) except the left-handed d-type quarks, for which the usual relation between the weak and mass eigenstates reads [76]

$$d_{Lm}^{(\text{weak})} = V_{md}P_L d^{(\text{mass})} + V_{ms}P_L s^{(\text{mass})}$$
$$+ V_{mb}P_L b^{(\text{mass})} \equiv \sum_n V_{mn}P_L d_n^{(\text{mass})}, \tag{2.8}$$

where $P_{R,L} \equiv \frac{1\pm\gamma_5}{2}$ are the right- and left-handed chiral projectors. As we are concerned mainly on the operators $Q_{lq}^{(3)}$, $Q_{ledq}, Q_{lequ}^{(1)}$ and $Q_{lequ}^{(3)}$, as well as their hermitian conjugates, the effective quark-mixing matrix V appearing in Eq. (2.8) coincides with the SM CKM matrix.

The second step is to perform the matching at the EW scale μ_{EW}. After integrating out the SM heavy particles, the $W^\pm$, Z^0, the top quark, and the Higgs boson, we can obtain the WET Lagrangian suitable for describing the $b \rightarrow c\tau\nu$ transitions [75,76,79]

$$\mathcal{L}_{\text{WET}} = \mathcal{L}_{\text{QCD+QED}}^{(u,d,c,s,b,e,\mu,\tau,\nu_e,\nu_\mu,\nu_\tau)} + \mathcal{L}_{\text{SM}}^{(6)} + \mathcal{L}_{\text{NP}}^{(6)}, \tag{2.9}$$

where $\mathcal{L}_{\text{QCD+QED}}^{(u,d,c,s,b,e,\mu,\tau,\nu_e,\nu_\mu,\nu_\tau)}$ is the QCD and QED Lagrangian with all the six leptons and the five lightest quarks as the active degrees of freedom for fermions, and

$$\mathcal{L}_{\text{SM}}^{(6)} = -\frac{4G_F}{\sqrt{2}} V_{cb} \mathcal{O}_{V_L} + \text{h.c.}, \tag{2.10}$$

$$\mathcal{L}_{\text{NP}}^{(6)} = -\frac{4G_F}{\sqrt{2}} V_{cb} \left(C_{V_L}\mathcal{O}_{V_L}\right.$$
$$\left. + C_{V_R}\mathcal{O}_{V_R} + C_{S_L}\mathcal{O}_{S_L} + C_{S_R}\mathcal{O}_{S_R} + C_T\mathcal{O}_T\right) + \text{h.c.}, \tag{2.11}$$

with the WET dimension-six operators given, respectively, by[5]

$$\mathcal{O}_{V_{L(R)}} = (\bar{c}\gamma^\mu P_{L(R)}b)(\bar{\tau}\gamma_\mu P_L \nu),$$
$$\mathcal{O}_{S_{L(R)}} = (\bar{c}P_{L(R)}b)(\bar{\tau}P_L \nu),$$
$$\mathcal{O}_T = (\bar{c}\sigma^{\mu\nu}P_L b)(\bar{\tau}\sigma_{\mu\nu}P_L \nu). \tag{2.12}$$

---

[5] Neutrinos are assumed to be left-handed throughout this paper and, hence, we need not consider the tensor operator $(\bar{c}\sigma^{\mu\nu}P_R b)(\bar{\tau}\sigma_{\mu\nu}P_L \nu)$, which is obtained from $\mathcal{O}_T$ by changing the chirality of the quark current, because it is identically zero due to Fierz transformations.

Matching at tree level the SMEFT operators given by Eq. (2.2) onto the WET ones given by Eq. (2.12) at the scale μ_{EW}, we get [76,79]

$$C_{V_L} = -\frac{\sqrt{2}}{2G_F\Lambda^2} \sum_n \left[C_{lq}^{(3)}\right]_{332n} \frac{V_{nb}}{V_{cb}},$$

$$C_{S_R} = -\frac{\sqrt{2}}{4G_F\Lambda^2} \frac{1}{V_{cb}} \left[C_{ledq}\right]_{3332}^*,$$

$$C_{S_L} = -\frac{\sqrt{2}}{4G_F\Lambda^2} \sum_n \left[C_{lequ}^{(1)}\right]_{33n2}^* \frac{V_{nb}}{V_{cb}},$$

$$C_T = -\frac{\sqrt{2}}{4G_F\Lambda^2} \sum_n \left[C_{lequ}^{(3)}\right]_{33n2}^* \frac{V_{nb}}{V_{cb}}. \tag{2.13}$$

Here we do not consider the Wilson coefficient C_{V_R}, because it is explicitly lepton-flavour universal in the SMEFT formalism, up to contributions of $\mathcal{O}(\mu_{EW}^4/\Lambda^4)$ [76,79,85–87]. We shall also neglect terms proportional to the small CKM factors V_{ub} and V_{cb} [88], corresponding to $n = 1$ and $n = 2$, respectively. In such a case, the $b \to c\tau\nu$ transitions can only be affected by the Wilson coefficients $\left[C_{lq}^{(3)}\right]_{3323}$, $\left[C_{ledq}\right]_{3332}$, $\left[C_{lequ}^{(1)}\right]_{3332}$, and $\left[C_{lequ}^{(3)}\right]_{3332}$.

The last step is to evolve the WET Lagrangian $\mathcal{L}_{WET}$ from μ_{EW} down to μ_b under the gauge group $SU(3)_C \otimes U(1)_{em}$, with the corresponding RGEs given schematically by

$$\mu \frac{d\overrightarrow{\mathcal{C}}}{d\mu} = \left[\frac{\alpha_e}{4\pi}\gamma_{em} + \sum_{k=1}^3 \left(\frac{\alpha_s}{4\pi}\right)^k \gamma_s^{(k)}\right] \cdot \overrightarrow{\mathcal{C}}, \tag{2.14}$$

where $\overrightarrow{\mathcal{C}} = (C_{V_L}, C_{S_R}, C_{S_L}, C_T)$, and $\alpha_e = e^2/(4\pi)$ and $\alpha_s = g_s^2/(4\pi)$ are the electromagnetic and strong coupling constants, respectively. The non-zero elements of the one-loop electromagnetic anomalous dimension matrix γ_{em} read [75,77,82,89–91]

$$[\gamma_{em}]_{11} = -4, \quad [\gamma_{em}]_{22} = \frac{4}{3}, \quad [\gamma_{em}]_{33} = \frac{4}{3},$$

$$[\gamma_{em}]_{34} = 8, \quad [\gamma_{em}]_{43} = \frac{1}{6}, \quad [\gamma_{em}]_{44} = -\frac{40}{9}. \tag{2.15}$$

The QCD anomalous dimension matrices $\gamma_s^{(k)}$ are known to three loops, with all the non-zero entries given by [75,77,82, 92,93]

$$\left[\gamma_s^{(1)}\right]_{22} = \left[\gamma_s^{(1)}\right]_{33} = -8, \quad \left[\gamma_s^{(1)}\right]_{44} = \frac{8}{3},$$

$$\left[\gamma_s^{(2)}\right]_{22} = \left[\gamma_s^{(2)}\right]_{33} = \frac{4}{9}(-303 + 10n_f),$$

$$\left[\gamma_s^{(2)}\right]_{44} = \frac{4}{27}(543 - 26n_f),$$

$$\left[\gamma_s^{(3)}\right]_{22} = \left[\gamma_s^{(3)}\right]_{33}$$

$$= \frac{2}{81}[-101169 + 24(277 + 180\zeta_3)n_f + 140n_f^2],$$

$$\left[\gamma_s^{(3)}\right]_{44} = \frac{2}{81}[52555 - 2784\zeta_3 - 40(131 + 36\zeta_3)n_f - 36n_f^2]. \tag{2.16}$$

As the reference energy scale in $b \to c\tau\nu$ transitions is at around $\mu_b \simeq 5$ GeV, the RGE from μ_{EW} down to μ_b does not involve crossing any threshold, and the effective number of quark flavours n_f can be fixed at $n_f = 5$.

There exist several ready-made packages, such as `Wilson` [78] and `DsixTools` [94], to implement the evolution using the full one-loop anomalous dimension matrices as well as the tree-level matching. In our numerical analysis, we shall work at three-loop in QCD and one-loop in EW/QED, together with the same order for the corresponding coupling constants α_s, g, g' and α_e.

3 Observables in $b \to c\tau\nu$ transitions

3.1 $B \to D^{(*)}\tau\nu$

There have been a lot of calculations for the differential decay rates of $B \to D^{(*)}\tau\nu$ in the presence of all the operators given in Eq. (2.12). In this paper, we shall follow the analytical expressions given in Refs. [95–97], and consider the following observables:

- q^2-dependent and q^2-integrated ratios

$$R_{D^{(*)}}(q^2) = \frac{d\Gamma(B \to D^{(*)}\tau\nu)/dq^2}{d\Gamma(B \to D^{(*)}\ell\nu)/dq^2}, \quad \text{and}$$

$$R(D^{(*)}) = \frac{\mathcal{B}(B \to D^{(*)}\tau\nu)}{\mathcal{B}(B \to D^{(*)}\ell\nu)}, \tag{3.1}$$

where, on the theoretical side, we define

$$d\Gamma(B \to D^{(*)}\ell\nu)/dq^2 = \frac{1}{2}\left[d\Gamma(B \to D^{(*)}\mu\nu)/dq^2 + d\Gamma(B \to D^{(*)}e\nu)/dq^2\right],$$

$$\mathcal{B}(B \to D^{(*)}\ell\nu) = \frac{1}{2}\left[\mathcal{B}(B \to D^{(*)}\mu\nu) + \mathcal{B}(B \to D^{(*)}e\nu)\right].$$

- τ forward–backward asymmetry

$$A_{FB}^{D^{(*)}}(q^2)$$

$$= \frac{\left(\int_0^1 - \int_{-1}^0\right) d\cos\theta \left[d^2\Gamma(B \to D^{(*)}\tau\nu)/\left(dq^2 d\cos\theta\right)\right]}{d\Gamma(B \to D^{(*)}\tau\nu)/dq^2}, \tag{3.2}$$

where θ is the angle between the three-momenta of the τ lepton and the B meson in the $\tau\nu$ rest frame.

- τ spin polarization

$$P_\tau^{D^{(*)}}(q^2)$$
$$= \frac{d\Gamma^{\lambda_\tau=1/2}(B \to D^{(*)}\tau\nu)/dq^2 - d\Gamma^{\lambda_\tau=-1/2}(B \to D^{(*)}\tau\nu)/dq^2}{d\Gamma(B \to D^{(*)}\tau\nu)/dq^2},$$
$$(3.3)$$

which can be inferred from the distinctive τ decay patterns.

- D^* longitudinal and transverse polarizations

$$P_L^{D^*}(q^2) = \frac{d\Gamma^{\lambda_{D^*}=0}(B \to D^*\tau\nu)/dq^2}{d\Gamma(B \to D^*\tau\nu)/dq^2}, \quad \text{and}$$
$$P_T^{D^*}(q^2) = 1 - P_L^{D^*}(q^2), \quad (3.4)$$

which can be measured by fitting to the double differential decay distribution or from the D^* decays.

Integrating separately the numerator and denominator in Eqs. (3.2)–(3.4) over the whole interval of the momentum transfer squared, $m_\tau^2 \leq q^2 \leq (m_B - m_{D^{(*)}})^2$, we can get the q^2-integrated observables $A_{FB}(D^{(*)})$, $P_\tau(D^{(*)})$, $P_L(D^*)$, and $P_T(D^*)$, respectively.

In analogy to the ratios $R(D^{(*)})$, we can also define the following observables with the denominators involving only the light-lepton modes:

- τ forward and backward fractions

$$\mathcal{X}_{1,2}(D^{(*)}) = \frac{1}{2}R(D^{(*)})[1 \pm A_{FB}(D^{(*)})]. \quad (3.5)$$

- τ spin $1/2$ and $-1/2$ fractions

$$\mathcal{X}_{3,4}(D^{(*)}) = \frac{1}{2}R(D^{(*)})[1 \pm P_\tau(D^{(*)})]. \quad (3.6)$$

- D^* longitudinal and transverse polarization fractions

$$\mathcal{X}_5(D^*) = R(D^*)P_L(D^*), \quad (3.7)$$
$$\mathcal{X}_6(D^*) = R(D^*)P_T(D^*) = R(D^*)\left[1 - P_L(D^*)\right]. \quad (3.8)$$

It is important to note that in our scenario (i.e. only the third-generation leptons are affected by the NP contributions) these observables are not independent. However, because of the different normalization and systematics, future measurements of them would provide important information on the size and nature of NP in $B \to D^{(*)}\tau\nu$ decays.

In our calculation, the $B \to D^{(*)}$ transition form factors are taken from Ref. [16], in which both $\mathcal{O}(\Lambda_{QCD}/m_{b,c})$ and

$\mathcal{O}(\alpha_s)$ corrections in the heavy quark effective theory are included.

3.2 $\Lambda_b \to \Lambda_c\tau\nu$

For an unpolarized Λ_b, the twofold angular distribution for $\Lambda_b \to \Lambda_c\tau\nu$ can be written as [98–100]

$$\frac{d^2\Gamma}{dq^2 d\cos\theta_\tau}$$
$$= \frac{G_F^2|V_{cb}|^2}{2}\frac{v^2|\mathbf{p}_{\Lambda_c}|}{256\pi^3 m_{\Lambda_b}^2}\sum_{\lambda_{\Lambda_c}}\sum_{\lambda_\tau}\frac{1}{2}\sum_{\lambda_{\Lambda_b}}|\mathcal{M}_{\lambda_{\Lambda_b}}^{\lambda_{\Lambda_c},\lambda_\tau}|^2, \quad (3.9)$$

where $v = \sqrt{1 - m_\tau^2/q^2}$, and $|\mathbf{p}_{\Lambda_c}| = \sqrt{Q_+Q_-}/(2m_{\Lambda_b})$ is the magnitude of the Λ_c three-momentum in the Λ_b rest frame, with $Q_\pm = (m_{\Lambda_b} \pm m_{\Lambda_c})^2 - q^2$, while θ_τ is the angle between the three-momenta of the τ lepton and the Λ_c baryon in the $\tau\nu$ rest frame. The helicity amplitudes $\mathcal{M}_{\lambda_{\Lambda_b}}^{\lambda_{\Lambda_c},\lambda_\tau}$, with the indices λ_{Λ_b}, λ_{Λ_c} and λ_τ denoting respectively the helicities of the Λ_b, Λ_c baryons and the τ lepton, can be calculated by following the helicity method described in Refs. [101–104]; for convenience, their explicit expressions are given in the "Appendix".

The observables of this process we are considering include

- q^2-dependent and q^2-integrated ratios

$$R_{\Lambda_c}(q^2) = \frac{d\Gamma(\Lambda_b \to \Lambda_c\tau\nu)/dq^2}{d\Gamma(\Lambda_b \to \Lambda_c\mu\nu)/dq^2}, \quad \text{and}$$
$$R(\Lambda_c) = \frac{\mathcal{B}(\Lambda_b \to \Lambda_c\tau\nu)}{\mathcal{B}(\Lambda_b \to \Lambda_c\mu\nu)}. \quad (3.10)$$

- τ forward–backward asymmetry

$$A_{FB}^{\Lambda_c}(q^2)$$
$$= \frac{\left(\int_0^1 - \int_{-1}^0\right)d\cos\theta_\tau\left[d^2\Gamma(\Lambda_b \to \Lambda_c\tau\nu)/(dq^2 d\cos\theta_\tau)\right]}{d\Gamma(\Lambda_b \to \Lambda_c\tau\nu)/dq^2}. \quad (3.11)$$

- τ spin polarization

$$P_\tau^{\Lambda_c}(q^2)$$
$$= \frac{d\Gamma^{\lambda_\tau=1/2}(\Lambda_b \to \Lambda_c\tau\nu)/dq^2 - d\Gamma^{\lambda_\tau=-1/2}(\Lambda_b \to \Lambda_c\tau\nu)/dq^2}{d\Gamma(\Lambda_b \to \Lambda_c\tau\nu)/dq^2}. \quad (3.12)$$

- Λ_c spin polarization

$$P_{\Lambda_c}(q^2)$$
$$= \frac{d\Gamma^{\lambda_{\Lambda_c}=1/2}(\Lambda_b \to \Lambda_c\tau\nu)/dq^2 - d\Gamma^{\lambda_{\Lambda_c}=-1/2}(\Lambda_b \to \Lambda_c\tau\nu)/dq^2}{d\Gamma(\Lambda_b \to \Lambda_c\tau\nu)/dq^2}. \quad (3.13)$$

Integrating separately the numerator and denominator in Eqs. (3.11)–(3.13) over the whole interval $q^2 \in [m_\tau^2, (m_{\Lambda_b} - m_{\Lambda_c})^2]$, we can get the q^2-integrated observables $A_{\mathrm{FB}}(\Lambda_c)$, $P_\tau(\Lambda_c)$ and P_{Λ_c}, respectively. As in the mesonic case, we can also construct the following observables normalized by the corresponding muonic mode:

- τ forward and backward fractions

$$\mathcal{X}_{1,2}(\Lambda_c) = \frac{1}{2} R(\Lambda_c) \left[1 \pm A_{\mathrm{FB}}(\Lambda_c) \right]. \tag{3.14}$$

- τ spin 1/2 and −1/2 fractions

$$\mathcal{X}_{3,4}(\Lambda_c) = \frac{1}{2} R(\Lambda_c) \left[1 \pm P_\tau(\Lambda_c) \right]. \tag{3.15}$$

- Λ_c spin 1/2 and −1/2 fractions

$$\mathcal{X}_{5,6}(\Lambda_c) = \frac{1}{2} R(\Lambda_c) \left[1 \pm P_{\Lambda_c} \right]. \tag{3.16}$$

In our numerical analysis, we use the $\Lambda_b \to \Lambda_c$ transition form factors computed in lattice QCD including all the types of NP currents [100,105].

3.3 The rest observables

In this subsection, we introduce the rest observables relevant for $B_c \to (J/\psi, \eta_c)\tau\nu$, $B \to X_c\tau\nu$ and $B_c \to \tau\nu$ decays, which could provide additional constraints on the NP parameters.

3.3.1 $B_c \to (J/\psi, \eta_c)\tau\nu$

Similar to the definitions of $R(D^{(*)})$, the ratios $R(J/\psi)$ and $R(\eta_c)$ for $B_c \to (J/\psi, \eta_c)\tau\nu$ decays are defined, respectively, by

$$R(J/\psi) = \frac{\mathcal{B}(B_c \to J/\psi\tau\nu)}{\mathcal{B}(B_c \to J/\psi\mu\nu)},$$
$$R(\eta_c) = \frac{\mathcal{B}(B_c \to \eta_c\tau\nu)}{\mathcal{B}(B_c \to \eta_c\mu\nu)}. \tag{3.17}$$

Using the model-dependent calculations of $B_c \to (J/\psi, \eta_c)$ transition form factors [106–118], the SM central values of $R(J/\psi)$ and $R(\eta_c)$ vary within the ranges $0.24 - 0.30$ and $0.25 - 0.35$, respectively, with the former being lower than the LHCb measurement $R(J/\psi)^{\mathrm{exp}} = 0.71(17)(18)$ [119] by 1.7σ. Recently, model-independent bounds on $R(J/\psi)$ [120–122] and $R(\eta_c)$ [121–123] are also obtained by constraining the transition form factors through a combination of dispersive relations, heavy-quark relations at zero-recoil, and the limited existing form-factor determinations from lattice QCD [124,125], resulting in $0.20 \leq R(J/\psi) \leq 0.39$

[120] and $0.24 \leq R(\eta_c) \leq 0.34$ [123], both of which agree with the weighted averages of previous model predictions. Here we shall use the $B_c \to (J/\psi, \eta_c)$ transition form factors calculated in Ref. [110], which are consistent with the preliminary lattice QCD results [124,125] at all available q^2 points, but would result in lower central values of $R(J/\psi)$ and $R(\eta_c)$ [24].

3.3.2 $B \to X_c\tau\nu$

For the inclusive decay $B \to X_c\tau\nu$, we consider the ratio

$$R(X_c) = \frac{\mathcal{B}(B \to X_c\tau\nu)}{\mathcal{B}(B \to X_c\ell\nu)}. \tag{3.18}$$

The analytic expression of the total decay width within the SM is given by [126]

$$\Gamma^{\mathrm{SM}}(B \to X_c\tau\nu) = \Gamma_0 S_{\mathrm{em}}^2 \left[C_0^{(0)} + \frac{\alpha_s}{\pi} C_0^{(1)} + C_{\mu_\pi^2} \frac{\mu_\pi^2}{m_b^2} \right.$$
$$\left. + C_{\mu_G^2} \frac{\mu_G^2}{m_b^2} + C_{\rho_D^3} \frac{\rho_D^3}{m_b^3} + C_{\rho_{LS}^3} \frac{\rho_{LS}^3}{m_b^3} \right], \tag{3.19}$$

where $\Gamma_0 = \frac{G_F^2 |V_{cb}|^2 m_b^5}{192\pi^2}$, and S_{em} accounts for the short-distance electromagnetic correction to the SM four-fermion operator mediating the semi-leptonic decay [89,90]. The coefficients $C_0^{(0)}$ and $C_0^{(1)}$ represent the partonic-level contributions with the leading- and next-to-leading-order corrections in α_s, respectively; while $C_{\mu_\pi^2}$, $C_{\mu_G^2}$ and $C_{\rho_D^3}$, $C_{\rho_{LS}^3}$ account for contributions from the $1/m_b^2$ and $1/m_b^3$ corrections in the heavy-quark expansion, respectively. Explicit analytic expressions of $C_0^{(0)}$, $C_{\mu_\pi^2}$, $C_{\mu_G^2}$ and $C_{\rho_D^3}$ can be found, for example, in Refs. [126–128], whereas $C_{\rho_{LS}^3} \equiv 0$ [126]. The result of $C_0^{(1)}$ can be deduced, on the other hand, from Refs. [129–131]. The non-perturbative parameters μ_π^2, μ_G^2 and ρ_D^3, ρ_{LS}^3 are defined in terms of the forward matrix elements of dimension-five and -six operators, respectively. To calculate the ratio $R(X_c)$, we take [33,132]: $\mu_\pi^2 = 0.464(67)$ GeV^2, $\mu_G^2 = 0.333(61)$ GeV^2, $\rho_D^3 = 0.175(40)$ GeV^3, and $\rho_{LS}^3 = -0.146(96)$ GeV^3, with $m_b^{\mathrm{kin}}(1\mathrm{GeV}) = 4.561(21)$ GeV and $m_c^{\mathrm{kin}}(1\mathrm{GeV}) = 1.092(20)$ GeV in the kinetic scheme [133]; the correlations between these parameters [33,132] are also considered.

To discuss the NP effects from Eq. (2.9) on the inclusive $B \to X_c\tau\nu$ decay, we take the partonic-level approximation, and decompose the decay width as [134]

$$\Gamma(B \to X_c\tau\nu) = \Gamma^{\mathrm{SM}} + \Gamma_{(1)}^{\mathrm{NP}} + \Gamma_{(2)}^{\mathrm{NP}}, \tag{3.20}$$

where the first term arises solely from the SM and is given by Eq. (3.19), while $\Gamma_{(1)}^{\mathrm{NP}}$ and $\Gamma_{(2)}^{\mathrm{NP}}$ represent respectively the interference term with the SM as well as the term that is of second order in the NP couplings, explicit expressions of

which are taken from Ref. [134]. Some recent works, discussing NP effects in this inclusive mode, can be found in Refs. [126,135–140].

3.3.3 $B_c \to \tau\nu$

The decay $B_c \to \tau\nu$, despite being at the moment out of the experimental reach [141], can provide a powerful constraint on NP scenarios involving scalar operators [138,139,142,143]. In terms of the WET Lagrangian given by Eq. (2.9), its branching ratio can be written as

$$
\mathcal{B}(B_c \to \tau\nu) = \tau_{B_c} \frac{m_{B_c} m_\tau^2 f_{B_c}^2 G_F^2 |V_{cb}|^2}{8\pi} \left(1 - \frac{m_\tau^2}{m_{B_c}^2}\right)^2
$$
$$
\times \left| 1 + C_{V_L} - C_{V_R} + \frac{m_{B_c}^2}{m_\tau (\overline{m}_b + \overline{m}_c)} (C_{S_R} - C_{S_L}) \right|^2,
$$
(3.21)

where $\overline{m}_b$ and $\overline{m}_c$ are the bottom- and charm-quark running masses in the $\overline{\text{MS}}$ scheme evaluated at the scale μ_b. In our numerical analysis, we take as input the lifetime $\tau_{B_c} = 0.507(9)$ ps, the mass $m_{B_c} = 6.2751(10)$ GeV, and the decay constant $f_{B_c} = 0.434(15)$ GeV [144].

An upper bound obtained from the LEP data, $\mathcal{B}(B_c \to \tau\nu) \lesssim 10\%$ [143], is stronger than the conservative constraint, $\mathcal{B}(B_c \to \tau\nu) \lesssim 30\%$ [142], by demanding that the rate does not exceed the fraction of the total width allowed by the calculation of the B_c lifetime within the SM. Here we shall use the former in our numerical analysis.

4 Numerical results and discussions

Before presenting the numerical results, we firstly collect in Table 1 the remaining theoretical input parameters used throughout this paper. The CKM parameters are taken from Ref. [145], in which the leptonic and semi-leptonic decays involving the μ and τ leptons have been removed from the global fit to the CKM parameters, following the current experimental indications that the electronic modes are in agreement with the SM predictions.

4.1 Numerical effects of evolution and matching

In this subsection, we illustrate the numerical effects of the evolution and matching procedure, based on Eqs. (2.3)–(2.7) and (2.14)–(2.16). To this end, we firstly calculate the couplings α_s, g and g' at the initial scale Λ via their RGEs within the SM. Using Eqs. (2.3)–(2.7), we can then obtain the values of $\left[C_{lq}^{(3)}\right]_{3323}$, $\left[C_{ledq}\right]_{3332}$, $\left[C_{lequ}^{(1)}\right]_{3332}$ and $\left[C_{lequ}^{(3)}\right]_{3332}$ at the scale μ_{EW}. Performing the tree-level matching at the scale μ_{EW}, we can obtain the values of the Wilson coefficients associated with the WET operators, which can be finally run down to the scale μ_b by using Eqs. (2.14)–(2.16). Numerically, we have the following relations (for simplicity, the Wilson coefficients are all assumed to be real):

$$
C_{V_L}(\mu_b) = -1.503 \left[C_{lq}^{(3)}\right]_{3323}(\Lambda),
$$
(4.1)
$$
C_{V_R}(\mu_b) = 0,
$$
(4.2)
$$
C_{S_L}(\mu_b) = -1.257 \left[C_{lequ}^{(1)}\right]_{3332}(\Lambda)
$$
$$
+ 0.2076 \left[C_{lequ}^{(3)}\right]_{3332}(\Lambda),
$$
(4.3)
$$
C_{S_R}(\mu_b) = -1.254 \left[C_{ledq}\right]_{3332}(\Lambda),
$$
(4.4)
$$
C_T(\mu_b) = 0.002725 \left[C_{lequ}^{(1)}\right]_{3332}(\Lambda)
$$
$$
- 0.6059 \left[C_{lequ}^{(3)}\right]_{3332}(\Lambda),
$$
(4.5)

with $\mu_b = 4.18$ GeV and $\Lambda = 1$ TeV. At the same time, the SM effective Lagrangian $\mathcal{L}_{\text{SM}}^{(6)}$ given by Eq. (2.10) should be changed to $S_{\text{em}}\mathcal{L}_{\text{SM}}^{(6)}$, with $S_{\text{em}} \simeq 1.0075$ encoding the short-distance electromagnetic correction to the SM four-fermion operator [89,90]. It can be clearly seen from Eqs. (4.3) and (4.5) that there exists a large mixing of the tensor operator into the (pseudo)scalar ones under EW/QED interactions [80–82].

Table 1 Summary of the remaining theoretical input parameters used throughout this paper

QCD and electroweak parameters [146]				
$G_F[10^{-5} \text{ GeV}^{-2}]$	$\alpha_s(M_Z)$	$\alpha_e(M_W)$	$M_Z[\text{GeV}]$	$\sin^2\theta_W$
1.1663787(6)	0.1181(11)	1/128	91.1876(21)	0.23122(4)
Quark and lepton masses [GeV] [146]				
$\overline{m}_b(\overline{m}_b)$	$\overline{m}_c(\overline{m}_c)$	m_τ	m_μ	m_e
$4.18^{+0.04}_{-0.03}$	$1.275^{+0.025}_{-0.035}$	1.77686(12)	0.10566	5.10999×10^{-4}
CKM parameters [145]				
λ	A	$\overline{\rho}$	$\overline{\eta}$	
0.2251(4)	$0.831^{+0.021}_{-0.031}$	0.155(8)	0.340(10)	

Table 2 Predictions for the observables listed in Sect. 3 within the SM

$B \to D \tau \nu$						
$R(D)^{SM}$	$A_{FB}(D)^{SM}$	$P_\tau(D)^{SM}$	$\mathcal{X}_1(D)^{SM}$	$\mathcal{X}_2(D)^{SM}$	$\mathcal{X}_3(D)^{SM}$	$\mathcal{X}_4(D)^{SM}$
0.2989(33)	0.3597(3)	0.3222(22)	0.2032(22)	0.0957(11)	0.1976(24)	0.1013(10)
$B \to D^* \tau \nu$						
$R(D^*)^{SM}$	$A_{FB}(D^*)^{SM}$	$P_\tau(D^*)^{SM}$	$P_L(D^*)^{SM}$	$\mathcal{X}_1(D^*)^{SM}$	$\mathcal{X}_2(D^*)^{SM}$	$\mathcal{X}_3(D^*)^{SM}$
0.2572(29)	−0.0559(22)	−0.5039(37)	0.4552(31)	0.1214(13)	0.1358(17)	0.0638(8)
$\mathcal{X}_4(D^*)^{SM}$	$\mathcal{X}_5(D^*)^{SM}$	$\mathcal{X}_6(D^*)^{SM}$				
0.1934(23)	0.1171(14)	0.1401(19)				
$\Lambda_b \to \Lambda_c \tau \nu$						
$R(\Lambda_c)^{SM}$	$A_{FB}(\Lambda_c)^{SM}$	$P_\tau(\Lambda_c)^{SM}$	$P_{\Lambda_c}^{SM}$	$\mathcal{X}_1(\Lambda_c)^{SM}$	$\mathcal{X}_2(\Lambda_c)^{SM}$	$\mathcal{X}_3(\Lambda_c)^{SM}$
0.3328(101)	0.0244(76)	−0.3077(139)	−0.7588(125)	0.1705(49)	0.1623(55)	0.1152(37)
$\mathcal{X}_4(\Lambda_c)^{SM}$	$\mathcal{X}_5(\Lambda_c)^{SM}$	$\mathcal{X}_6(\Lambda_c)^{SM}$				
0.2176(75)	0.0401(27)	0.2927(86)				
The rest observables						
$R(J/\psi)^{SM}$		$R(\eta_c)^{SM}$		$R(X_c)^{SM}$	$\mathcal{B}(B_c \to \tau \nu)^{SM}$	
$0.2483^{+0.0060}_{-0.0055}$		$0.2813^{+0.0181}_{-0.0153}$		0.2138(44)	$2.37^{+0.21}_{-0.24}\%$	

The numerical relations given by Eqs. (4.1)–(4.5) allow us to connect the values of the SMEFT Wilson coefficients at the NP scale $\Lambda = 1$ TeV to that of the WET ones at the scale $\mu_b = 4.18$ GeV. In order to directly use the theoretical expressions of the observables listed in Sect. 3, which are all given in terms of the WET Wilson coefficients at the scale μ_b, we need only replace Eq. (4.1) by $C_{V_L}(\mu_b) = (S_{em} - 1) - 1.503 \left[C_{lq}^{(3)} \right]_{3323} (\Lambda)$, making the EW/QED evolution of the SM four-fermion operator also taken into account. In the following discussions, we shall use the abbreviations

$$C_1 \equiv \left[C_{lq}^{(3)} \right]_{3323} (\Lambda), \qquad C_2 \equiv \left[C_{ledq} \right]_{3332} (\Lambda),$$
$$C_3 \equiv \left[C_{lequ}^{(1)} \right]_{3332} (\Lambda), \qquad C_4 \equiv \left[C_{lequ}^{(3)} \right]_{3332} (\Lambda), \qquad (4.6)$$

for the sake of brevity.

4.2 SM results and comparison with data

Our predictions for the observables listed in Sect. 3 within the SM are collected in Table 2. The values of observables for $B \to D^{(*)} \tau \nu$ decays are always obtained by averaging over the charged and neutral modes. Although the relations $\mathcal{X}_i(\mathcal{H}) + \mathcal{X}_{i+1}(\mathcal{H}) = R(\mathcal{H})$ ($i = 1, 3$ for $\mathcal{H}$ is D, D^* or Λ_c, and $i = 5$ for $\mathcal{H}$ is D^* or Λ_c) hold, we are still presenting all of them in Table 2, because these observables involve different normalization and systematics and can, therefore, provide complementary information on the NP scenarios. This is clearly indicated by the reduced uncertainties of the observables $\mathcal{X}_i(\mathcal{H})$ compared to that of $R(\mathcal{H})$.

Among the observables listed in Table 2, the following ones have been measured: $R(D)^{exp} = 0.407(39)(24)$ and

$R(D^*)^{exp} = 0.306(13)(7)$ with a correlation of -0.203 [14], $P_\tau(D^*)^{exp} = -0.38^{+0.51+0.21}_{-0.51-0.16}$ [8], $R(J/\psi)^{exp} = 0.71(17)(18)$ [119], and $R(X_c)^{exp} = 0.220(22)$.[6] The differences between the experimental measurements and the SM predictions (ΔObs. $=$ Obs.^{exp} − Obs.^{SM}) for these observables read: $\Delta R(D) = 0.1081(459)$ and $\Delta R(D^*) = 0.0488(150)$ with a correlation of -0.199, $\Delta P_\tau(D^*) = 0.1239(5500)$, $\Delta R(J/\psi) = 0.4617(2477)$, and $\Delta R(X_c) = 0.0062(224)$. These discrepancies will be used to constrain the SMEFT Wilson coefficients.

4.3 Constraints on the SMEFT Wilson coefficients

In this subsection, we shall use $\Delta R(D)$, $\Delta R(D^*)$, $\Delta P_\tau(D^*)$, $\Delta R(J/\psi)$, and $\Delta R(X_c)$ to constrain the SMEFT Wilson coefficients C_{1-4} (see Eq. (4.6)). Firstly, we show in Fig. 1 the contributions to these observables in the presence of only a single C_i. It can be seen that, after taking into account the constraint $\mathcal{B}(B_c \to \tau \nu) \lesssim 10\%$, the scenario with a single C_3 is already ruled out by $\Delta R(D^{(*)})$ at 3σ (99.73% C.L.), and a single C_2 can be used to explain the $R(D^{(*)})$ anomalies only marginally at about 2σ (95.45% C.L.), while a single C_1

---

[6] This value is obtained by using the world average for the semi-leptonic branching fractions into the light leptons, $\mathcal{B}(B \to X_c \ell \nu) = (10.65 \pm 0.16)\%$ [146], and an averaged constraint from LEP, $\mathcal{B}(b \to X \tau \nu) = (2.41 \pm 0.23)\%$ [146], which is dominated by $b \to X_c \tau \nu$ because of $|V_{ub}|^2/|V_{cb}|^2 \sim 1\%$ and, after correcting for the $b \to u$ contribution that is about 2% due to the larger available phase space, is reduced to $\mathcal{B}(b \to X_c \tau \nu) = (2.35 \pm 0.23)\%$ [139]. It should be noted that the LEP measurement corresponds to a known admixture of initial states for the weak decay [147]. The inclusive decay rate does, however, not depend on this admixture to leading order in $1/m_b$. The corrections to this limit are hadron-specific and only partly known [127,135].
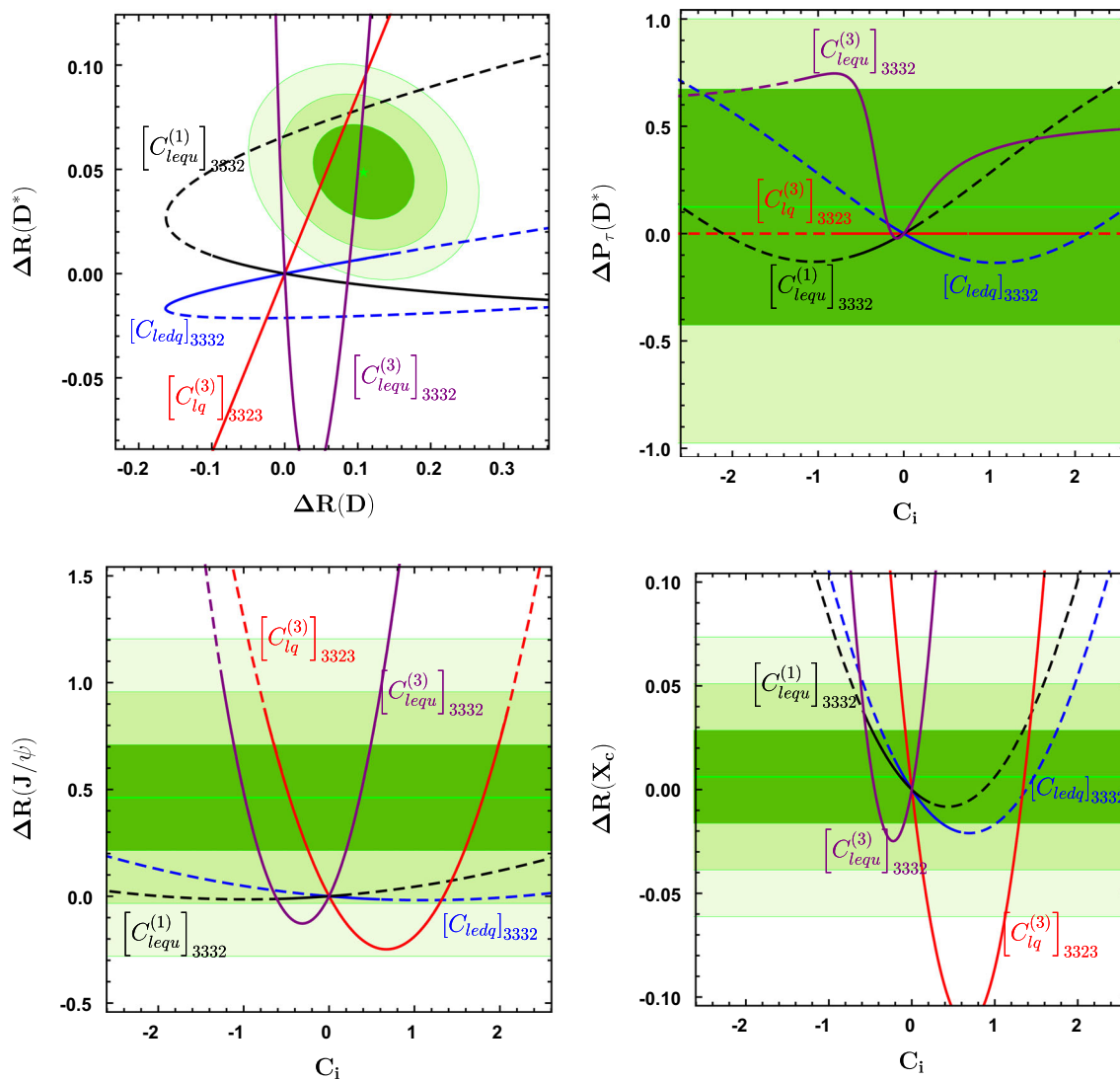
Fig. 1 Contributions to the observables in the presence of a single SMEFT Wilson coefficients C_i (see Eq. (4.6)). The red, blue, black, and purple lines stand for the contributions from C_1, C_2, C_3, and C_4, respectively, with the dashed parts being already ruled out by the constraint $\mathcal{B}(B_c \to \tau\nu) \lesssim 10\%$. The dark-green, green, and light-green areas represent the 1-, 2-, and 3-σ differences between the measurements and the SM predictions for the observables, respectively

or C_4 can provide a resolution of the $R(D^{(*)})$ anomalies at 1σ (68.27% C.L.), especially with the finding that the central values of the current world averages of $R(D^{(*)})$ can be well reproduced with a single C_4.

Due to the large experimental uncertainty of $P_\tau(D^*)$, the constraint $\Delta P_\tau(D^*)$ on the NP Wilson coefficients is quite weak. It can be seen from the upper-right plot of Fig. 1 that, with the constraint $\mathcal{B}(B_c \to \tau\nu) \lesssim 10\%$ taken into account, only C_4 has a significant impact on $\Delta P_\tau(D^*)$. Future more precise measurements of $P_\tau(D^*)$ at, for example, Belle II [148] will be, therefore, very helpful to discriminate between the C_1 and C_4 scenarios, both of which have been found to provide reasonable explanations of the $R(D^{(*)})$ anomalies

while satisfying the constraint $\mathcal{B}(B_c \to \tau\nu) \lesssim 10\%$. Using the constraints $\Delta R(J/\psi)$ and $\Delta R(X_c)$, on the other hand, we can further exclude some allowed intervals of C_1 and C_4 at 99.73% C.L., which do not however affect the upper-left plot of Fig. 1. The constraint from $\Delta R(X_c)$ is also found to be stronger than that from $\Delta R(J/\psi)$.

In the case where two NP Wilson coefficients are present simultaneously, we show in Fig. 2 the allowed regions in the (C_i, C_j) planes under the separate constraint from $\Delta R(D^{(*)})$, $\Delta R(J/\psi)$, and $\Delta R(X_c)$, all being varied within 3σ, as well as from the upper bound $\mathcal{B}(B_c \to \tau\nu) \lesssim 10\%$. As the experimental uncertainty is still quite large, we do not impose the constraint from $\Delta P_\tau(D^*)$ in this figure. It
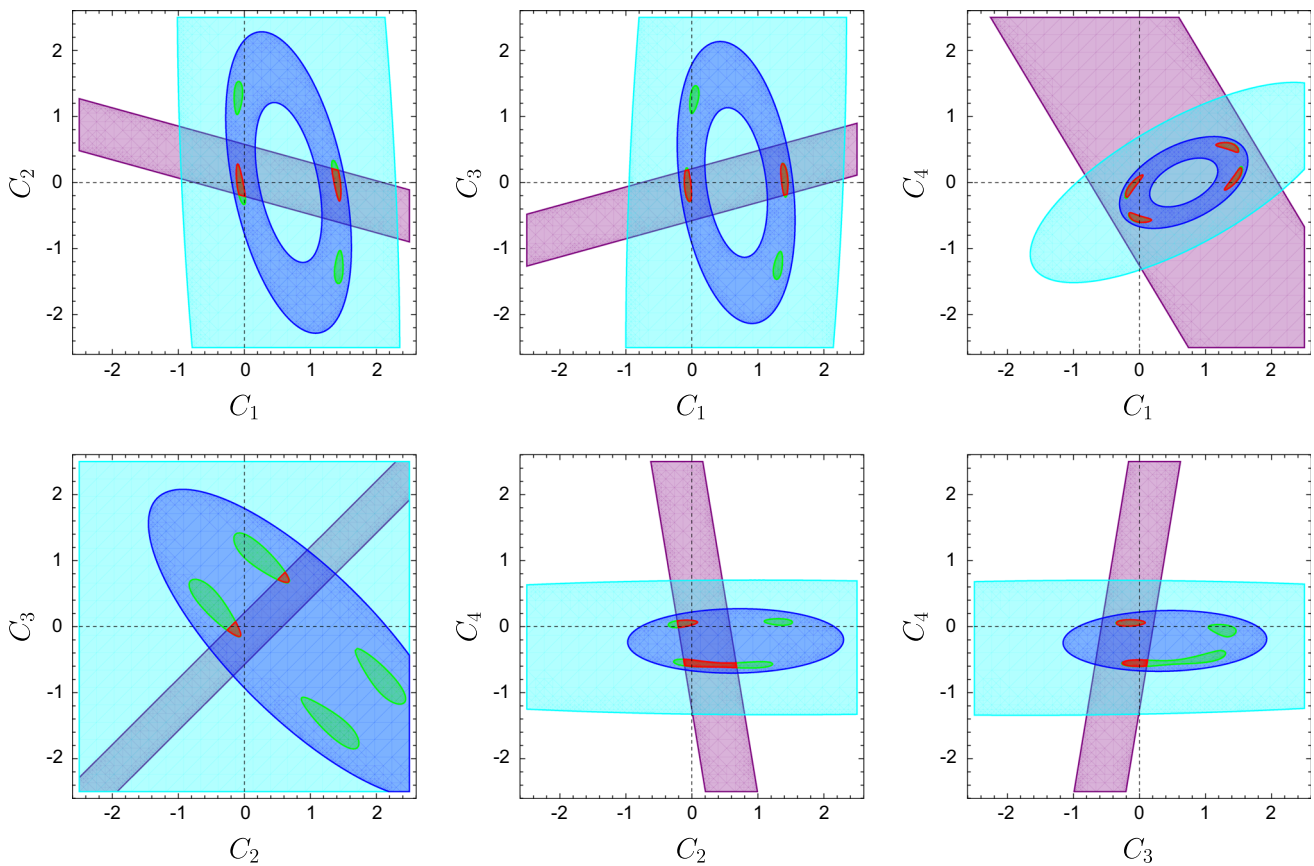
Fig. 2 Constraints on the NP Wilson coefficients in the simultaneous presence of two C_is. The green, cyan, and blue areas are allowed respectively by $\Delta R(D^{(*)})$, $\Delta R(J/\psi)$, and $\Delta R(X_c)$, all being varied within the 3σ range of their respective experimental data, while the purple bands are allowed by the upper bound $\mathcal{B}(B_c \to \tau\nu) \lesssim 10\%$. The red regions are obtained by requiring $\Delta \chi^2 \leq 11.83$ near the corresponding best-fit points given in Table 3, under the combined constraints from the measured $R(D)$, $R(D^*)$, $P_\tau(D^*)$, $R(J/\psi)$, and $R(X_c)$, being also compatible with the $\mathcal{B}(B_c \to \tau\nu) \lesssim 10\%$ constraint. With such a treatment, all coloured areas (except the purple ones) correspond to 99.73% C.L. regions

is found that, among all these constraints, the ones from $\Delta R(D)$ and $\Delta R(D^*)$ are the strongest, but the one from $\mathcal{B}(B_c \to \tau\nu) \lesssim 10\%$ is very complementary to them, making parts of the regions allowed by $\Delta R(D^{(*)})$ already excluded. It can also be seen that the $\mathcal{B}(B_c \to \tau\nu)$ constraint in the (C_2, C_3) plane is stronger than in the other five cases.

In order to constrain the NP Wilson coefficients C_i under the combined constraints from the measured $R(D)$, $R(D^*)$, $P_\tau(D^*)$, $R(J/\psi)$, and $R(X_c)$, we construct the usual χ^2 function:

$$\chi^2(C_i) = \mathcal{V}(C_i) \, \text{Cov}[\Delta R(D), \Delta R(D^*)]^{-1} \, \mathcal{V}^T(C_i)$$
$$+ \sum_{O = P_\tau(D^*), \, R(J/\psi), \, R(X_c)} \frac{\left(O^{\text{NP}}(C_i) - \Delta O\right)^2}{\sigma^2_{\Delta O}},$$
$$(4.7)$$

where $\mathcal{V}(C_i) = [R(D)^{\text{NP}}(C_i) - \Delta R(D), R(D^*)^{\text{NP}}(C_i) - \Delta R(D^*)]$, and $\text{Cov}[\Delta R(D), \Delta R(D^*)] = \text{Cov}[R(D)^{\text{exp}},$

$R(D^*)^{\text{exp}}] + \text{Cov}[R(D)^{\text{SM}}, R(D^*)^{\text{SM}}]$ is the covariance matrix between $\Delta R(D)$ and $\Delta R(D^*)$, the numerical value of which can be calculated by using the variance and correlation of $\Delta R(D)$ and $\Delta R(D^*)$ given in Sect. 4.2. Here we take in the fitting the averaged values of $R(D^{(*)})$ over the separate measurements by different experimental groups [4–12], as compiled by HFLAV [14].

By minimizing the $\chi^2(C_i)$ function in different scenarios, we can get the corresponding best-fit solutions, the results of which are shown in Table 3. Here the first column shows all possible cases with either a single C_i or a combination of two C_is, in addition to the SM case. The second column gives the values of χ^2_{min} with respect to different numbers of degrees of freedom (dof), with the corresponding best-fit points as well as the 1σ ranges ($\Delta \chi^2 = \chi^2(C_i) - \chi^2_{min} \leq 1$) for the single-parameter fits shown in the third column. Only the cases satisfying the condition $\chi^2_{min} \simeq$ dof are selected as the most possible solutions and are marked by different scenarios in the fourth column. In this way, we obtain eleven

Table 3 Best-fit solutions of the NP Wilson coefficients C_i at the scale $\Lambda = 1$ TeV, under the combined constraints from the measured $R(D)$, $R(D^*)$, $P_\tau(D^*)$, $R(J/\psi)$, and $R(X_c)$. See text for details

NP scenario	χ^2_{min}/dof	Best-fit point	Index	99.73% C.L. and $\mathcal{B}(B_c \to \tau\nu) \lesssim 10\%$
SM ($C_i = 0$)	23.5/5			
C_1	4.40/4	$-0.0679(150)$	S1	$-0.1111 \to -0.0220$
	4.40/4	$1.408(150)$	S2	$1.362 \to 1.452$
C_2	10.46/4	$-0.2198(546)$		$-0.2087 \to -0.0423$
C_3	17.12/4	$-0.1814(655)$		$-0.3481 \to 0.0425$
C_4	6.51/4	$-0.5571(148)$	S3	$-0.5979 \to -0.5101$
	9.14/4	$0.0611(149)$		$0.0139 \to 0.1020$
(C_1, C_2)	3.59/3	$(-0.0554, -0.0781)$	S4	The red areas shown in Fig. 2
	3.59/3	$(1.396, 0.0781)$	S5	
(C_1, C_3)	3.62/3	$(-0.0627, -0.0658)$	S6	
	3.62/3	$(1.403, 0.0658)$	S7	
(C_1, C_4)	3.79/3	$(-0.0962, -0.0352)$	S8	
	3.79/3	$(1.437, 0.0352)$	S9	
	6.51/3	$(0.0003, -0.5572)$		
	6.51/3	$(1.340, 0.5572)$		
(C_2, C_3)	3.50/3	$(-0.5169, 0.3580)$		
	3.19/3	$(0.1919, 1.109)$		
(C_2, C_4)	3.38/3	$(-0.1632, 0.0471)$	S10	
	6.06/3	$(0.9467, -0.5814)$		
	6.51/3	$(-0.0020, -0.5570)$		
(C_3, C_4)	3.38/3	$(-0.1643, 0.0596)$	S11	
	6.51/3	$(-0.0028, -0.5571)$		

most trustworthy scenarios, each of which can provide a good explanation of the $R(D^{(*)})$ anomalies at 1σ. The best-fit points allowed by $\Delta\chi^2 \leq 9$ (for the single-parameter fits) or $\Delta\chi^2 \leq 11.83$ (for the two-parameters fits) as well as by the upper bound $\mathcal{B}(B_c \to \tau\nu) \lesssim 10\%$ are finally represented in the fifth column. It is found that, after taking into account the combined constraints from $\Delta P_\tau(D^*)$, $\Delta R(J/\psi)$, and $\Delta R(X_c)$, the scenario with a single C_4 is no better than that with a single C_1 for resolving the $R(D^{(*)})$ anomalies.

4.4 Predictions for the observables in different NP scenarios

In order to further discriminate among the eleven most trustworthy scenarios obtained in the last subsection, we now calculate all the observables listed in Sect. 3 within these different scenarios. Our final numerical results are collected in Tables 4 and 5. During the calculation, we use the central values of the NP Wilson coefficients obtained in scenarios S1 to S11, and take into account the uncertainties caused by the input parameters.

From Tables 4 and 5, we can see that the scenarios S1 and S2, S4 and S5, S6 and S7, as well as S8 and S9, all of which involve the NP Wilson coefficient C_1 that would induce only

the left-handed vector current at the scale μ_b (see Eq. (4.1)), cannot be distinguished from each other. There are, however, a number of observables, such as $P_\tau(D)$, $\mathcal{X}_4(D)$, $A_{\text{FB}}(D^*)$, $P_\tau(D^*)$, $P_{\text{L}}(D^*)$, $\mathcal{X}_5(D^*)$, $P_\tau(\Lambda_c)$, P_{Λ_c}, and $\mathcal{X}_5(\Lambda_c)$, that can be used to distinguish the scenario S3 from the other ones. In addition to the scenario S3, there exist another two scenarios S10 and S11 that do not involve the Wilson coefficient C_1. As the predicted branching fraction of $B_c \to \tau\nu$ decay in the scenario S11 is much smaller than in the other scenarios as well as in the SM, we can use the observable $\mathcal{B}(B_c \to \tau\nu)$ to distinguish the scenario S11 from the other ones. On the other hand, the observables $P_\tau(D)$, $A_{\text{FB}}(D^*)$, $A_{\text{FB}}(\Lambda_c)$, $P_\tau(\Lambda_c)$, and $\mathcal{B}(B_c \to \tau\nu)$ have the potential to distinguish the scenario S10 from the other ones.

The scenarios S4, S5 and S6, S7 might be distinguished only by the observable $\mathcal{B}(B_c \to \tau\nu)$. While the observables $\mathcal{X}_i$ can help to distinguish the scenarios S1, S2 from the SM, the corresponding observables normalized by the tauonic modes, such as the τ forward-backward asymmetries $A_{\text{FB}}(D)$, $A_{\text{FB}}(D^*)$, and $A_{\text{FB}}(\Lambda_c)$, fail to do, because they are all identically the same in the scenarios S1 and S2 as well as in the SM.

In order to further differentiate these different scenarios, we now consider the correlations among the observables dis-

Table 4 Predictions for the observables involved in $B \to D^{(*)} \tau \nu$ decays in all the NP scenarios

| Obs.	S1, S2	S3	S4, S5	S6, S7	S8, S9	S10	S11
$R(D)$	0.3625(40)	0.3986(42)	0.4016(46)	0.4007(45)	0.3956(43)	0.4015(48)	0.4015(48)
$A_{\mathrm{FB}}(D)$	0.3597(3)	0.4297(4)	0.3485(4)	0.3504(4)	0.3695(4)	0.3130(5)	0.3072(4)
$P_\tau(D)$	0.3222(22)	0.0280(28)	0.4087(21)	0.3956(21)	0.3016(23)	0.5275(17)	0.5364(17)
$\mathcal{X}_1(D)$	0.2465(27)	0.2850(30)	0.2708(30)	0.2706(30)	0.2709(29)	0.2636(31)	0.2624(31)
$\mathcal{X}_2(D)$	0.1161(13)	0.1137(12)	0.1308(16)	0.1302(16)	0.1247(14)	0.1379(17)	0.1391(18)
$\mathcal{X}_3(D)$	0.2397(29)	0.2049(21)	0.2829(35)	0.2796(34)	0.2574(30)	0.3067(39)	0.3085(39)
$\mathcal{X}_4(D)$	0.1229(12)	0.1937(22)	0.1187(12)	0.1211(12)	0.1381(14)	0.0949(9)	0.0931(9)
$R(D^*)$	0.3119(35)	0.3042(43)	0.3049(35)	0.3050(35)	0.3057(35)	0.3057(34)	0.3058(35)
$A_{\mathrm{FB}}(D^*)$	−0.0559(22)	0.0312(15)	−0.0468(22)	−0.0634(22)	−0.0827(23)	0.0010(20)	−0.0280(20)
$P_\tau(D^*)$	−0.5039(37)	0.1808(33)	−0.4867(40)	−0.5176(33)	−0.5173(42)	−0.4432(37)	−0.4973(21)
$P_{\mathrm{L}}(D^*)$	0.4552(31)	0.1415(13)	0.4614(32)	0.4501(30)	0.4612(31)	0.4556(32)	0.4280(27)
$\mathcal{X}_1(D^*)$	0.1473(16)	0.1569(22)	0.1453(16)	0.1428(15)	0.1402(15)	0.1530(16)	0.1486(16)
$\mathcal{X}_2(D^*)$	0.1647(20)	0.1474(21)	0.1596(19)	0.1622(20)	0.1655(20)	0.1527(18)	0.1572(19)
$\mathcal{X}_3(D^*)$	0.0774(9)	0.1796(23)	0.0783(10)	0.0736(9)	0.0738(10)	0.0851(10)	0.0769(8)
$\mathcal{X}_4(D^*)$	0.2346(28)	0.1246(21)	0.2267(27)	0.2315(28)	0.2319(28)	0.2206(27)	0.2289(28)
$\mathcal{X}_5(D^*)$	0.1420(17)	0.0430(8)	0.1407(18)	0.1373(17)	0.1410(18)	0.1393(17)	0.1309(15)
$\mathcal{X}_6(D^*)$	0.1700(23)	0.2612(36)	0.1642(22)	0.1677(22)	0.1647(22)	0.1664(22)	0.1749(23)

Table 5 Predictions for the observables involved in $\Lambda_b \to \Lambda_c \tau \nu$ decay, as well as for $R(J/\psi)$, $R(\eta_c)$, $R(X_c)$, and $\mathcal{B}(B_c \to \tau\nu)$ in all the NP scenarios

Obs.	S1, S2	S3	S4, S5	S6, S7	S8, S9	S10	S11
$R(\Lambda_c)$	0.4037(123)	0.3646(247)	0.4085(125)	0.4090(125)	0.4107(123)	0.4044(130)	0.4043(133)
$A_{\mathrm{FB}}(\Lambda_c)$	0.0244(76)	0.1129(166)	0.0393(75)	0.0280(76)	0.0181(81)	0.0628(68)	0.0412(67)
$P_\tau(\Lambda_c)$	−0.3077(139)	0.1002(282)	−0.2487(155)	−0.2734(155)	−0.3076(145)	−0.1791(164)	−0.2108(169)
P_{Λ_c}	−0.7588(125)	0.1170(736)	−0.7570(117)	−0.7433(117)	−0.8031(111)	−0.6833(126)	−0.6188(127)
$\mathcal{X}_1(\Lambda_c)$	0.2068(59)	0.2029(155)	0.2123(62)	0.2102(61)	0.2091(59)	0.2149(66)	0.2104(66)
$\mathcal{X}_2(\Lambda_c)$	0.1969(67)	0.1617(98)	0.1962(67)	0.1988(68)	0.2016(68)	0.1895(66)	0.1938(69)
$\mathcal{X}_3(\Lambda_c)$	0.1397(45)	0.2006(155)	0.1535(53)	0.1486(52)	0.1422(47)	0.1660(61)	0.1595(61)
$\mathcal{X}_4(\Lambda_c)$	0.2640(91)	0.1641(114)	0.2551(88)	0.2604(89)	0.2685(91)	0.2384(85)	0.2447(89)
$\mathcal{X}_5(\Lambda_c)$	0.0487(32)	0.2037(249)	0.0496(31)	0.0525(32)	0.0404(28)	0.0640(37)	0.0770(41)
$\mathcal{X}_6(\Lambda_c)$	0.3550(104)	0.1610(107)	0.3589(106)	0.3565(105)	0.3703(108)	0.3404(105)	0.3272(102)
$R(J/\psi)$	$0.3012^{+0.0073}_{-0.0066}$	$0.1980^{+0.0215}_{-0.0167}$	$0.2939^{+0.0073}_{-0.0066}$	$0.2949^{+0.0069}_{-0.0064}$	$0.2935^{+0.0080}_{-0.0069}$	$0.2953^{+0.0067}_{-0.0064}$	$0.2971^{+0.0062}_{-0.0063}$
$R(\eta_c)$	$0.3412^{+0.0219}_{-0.0185}$	$0.3159^{+0.0304}_{-0.0261}$	$0.3766^{+0.0268}_{-0.0227}$	$0.3760^{+0.0264}_{-0.0223}$	$0.3692^{+0.0216}_{-0.0181}$	$0.3780^{+0.0324}_{-0.0277}$	$0.3788^{+0.0332}_{-0.0285}$
$R(X_c)$	0.2381(40)	0.2439(39)	0.2388(39)	0.2391(39)	0.2405(39)	0.2366(40)	0.2365(40)
$\mathcal{B}(B_c \to \tau\nu)[\%]$	$2.87^{+0.26}_{-0.29}$	$5.32^{+0.47}_{-0.54}$	$5.36^{+0.48}_{-0.55}$	$1.29^{+0.11}_{-0.13}$	$3.27^{+0.29}_{-0.33}$	$8.02^{+0.71}_{-0.82}$	$7.68^{+0.68}_{-0.78} \times 10^{-3}$

cussed in this paper. There are totally 465 correlation plots, with a small part of them shown in Fig. 3. As can be seen from the $R(D) - R(D^*)$ correlation plot, it is interesting to note that all the NP scenarios can resolve the $R(D^{(*)})$ anomalies at 1σ very well and, except in S1 and S2, the predicted $R(D^{(*)})$ in the other nine scenarios are very close to the center values of the current experimental data. The $R(D) - R(D^*)$ and $R(D) - \mathcal{X}_1(D)$ correlation plots have, therefore, the potential to distinguish the scenarios S1 and S2 from the other ones. Different patterns for different NP scenarios are also observed in the other correlation plots. For example, the $A_{\mathrm{FB}}(D) - P_\tau(D)$, $A_{\mathrm{FB}}(D) - \mathcal{X}_4(D)$, $\mathcal{X}_2(D) - \mathcal{X}_3(D)$, $A_{\mathrm{FB}}(D) - \mathcal{B}(B_c \to \tau\nu)$, and $P_\tau(D) - \mathcal{B}(B_c \to \tau\nu)$ correlation plots can be used to distinguish the scenarios S1 and S2 from the scenarios without C_1. The predicted patterns in the $P_\tau(D^*) - P_{\mathrm{L}}(D^*)$ and $A_{\mathrm{FB}}(D) - P_\tau(D^*)$ in the scenario S3 are also found to be very different from the ones in the other scenarios.

Based on all the above observations, we can, therefore, conclude that all the eleven NP scenarios, except S1 and
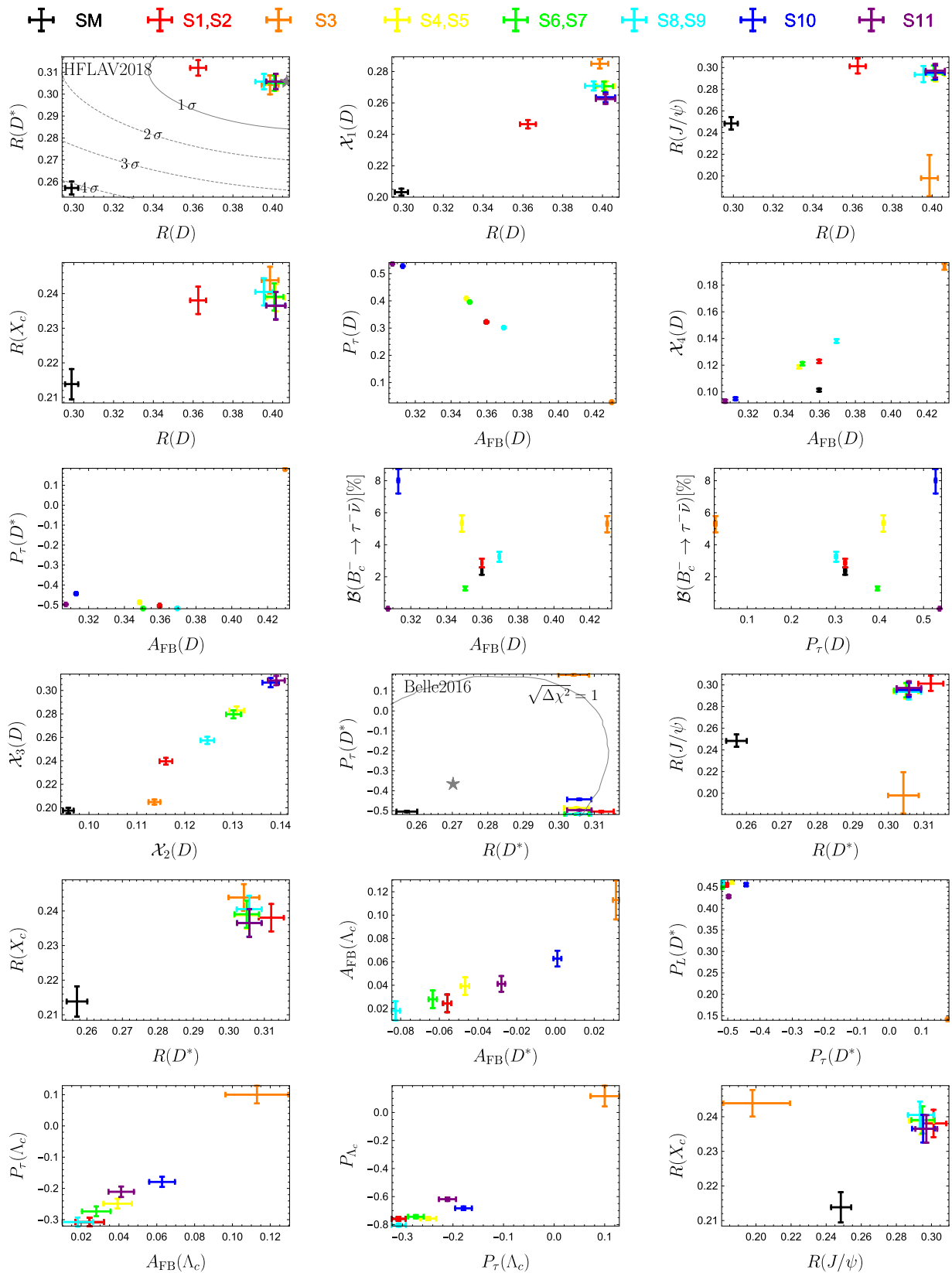
Fig. 3 Correlations among some of the observables discussed in this paper. Gray star point in the $R(D) - R(D^*)$ and $R(D^*) - P_\tau(D^*)$ plots correspond to the experimental central values

S2, S4 and S5, S6 and S7, as well as S8 and S9, can be distinguished from each other by the above observables as well as their correlations.

4.5 The $SU(2)_L$-invariant implications

Due to the $SU(2)_L$ invariance of the SMEFT Lagrangian, the non-zero Wilson coefficients C_{1-4} at the high-energy scale Λ enter not only in the $b \to c\tau\nu_\tau$ processes studied in this paper but also in other low-energy charged and/or neutral current processes [85,88,149]. With our prescription for the weak and mass eigenstates of fermion fields (see Eq. (2.8)), the processes $c \to d_n\tau\nu$, $d_m \to d_n\nu\bar{\nu}$ and $d_n \to d_m\tau^+\tau^-$, with d_m being one of the d-type quarks in the mass eigenstate, will also receive the NP contributions from C_{1-4}. However, compared with the $b \to c\tau\nu$ transitions, the NP effects on $c \to d_n\tau\nu$ ($d_n = d$ or s) processes are suppressed by the small factor $V_{cb}V_{tn}/V_{cn} \simeq 1.6 \times 10^{-3}$, and we can, therefore, neglect safely the NP impacts on the $D_{(s)}$-meson decays. On the other hand, it is found that the upper bound on the branching fraction of $B^+ \to K^+\nu\bar{\nu}$ decay given by the Belle [150] and BaBar [151] collaborations will disfavour the larger parameter regions for C_1 given in Table 3. Combining the χ^2-fit results with the constraint from the branching fraction of $B^+ \to K^+\nu\bar{\nu}$ [152–161], we also find that the C_1 contributions to the branching fractions of some $b \to s\tau^+\tau^-$ processes, such as $B_s \to \tau^+\tau^-$, $B \to K^{(*)}\tau^+\tau^-$, and $B_s \to \phi\tau^+\tau^-$ decays, can be enhanced by about two orders of magnitude compared to the SM [88]. The NP effects on $\Upsilon(nS) \to \tau^+\tau^-$ decays are, however, suppressed by the small factor $V_{cb}V_{ts}/V_{cs}$ compared to these $b \to s\tau^+\tau^-$ processes. Finally, it should be noted that there also exist some collider signals directly implied by the $R(D^{(*)})$ anomalies. For example, the partonic-level process $gc \to b\tau\nu$ implied by crossing symmetry from the $b \to c\tau\nu$ decay should also take place at the LHC [162]. Furthermore, the $\tau^+\tau^-$ resonance searches at the LHC [163,164] should also be confronted with what have been found in this paper [165]. Detailed analyses of the $SU(2)_L$-invariant implications will be presented in a forthcoming paper.

5 Conclusions

In this paper, we have discussed the $B \to D^{(*)}\tau\nu$, $\Lambda_b \to \Lambda_c\tau\nu$, $B_c \to (J/\psi, \eta_c)\tau\nu$, $B \to X_c\tau\nu$, and $B_c \to \tau\nu$ decays, all being mediated by the same quark-level $b \to c\tau\nu$ transition, in the SMEFT framework. First of all, we obtained the WET Lagrangian describing the $b \to c\tau\nu$ transitions at the scale $\mu_b = 4.18$ GeV, in terms of the Wilson coefficients of the SMEFT operators $C_1 \equiv \left[C_{lq}^{(3)}\right]_{3323}(\Lambda)$, $C_2 \equiv \left[C_{ledq}\right]_{3332}(\Lambda)$, $C_3 \equiv \left[C_{lequ}^{(1)}\right]_{3332}(\Lambda)$, and $C_4 \equiv$

$\left[C_{lequ}^{(3)}\right]_{3332}(\Lambda)$ given at the NP scale $\Lambda = 1$ TeV. This is achieved by using the RGEs at three-loop in QCD and one-loop in EW/QED based on Eqs. (2.3)–(2.7) and (2.14)–(2.16), as well as the tree-level matching of the SMEFT Lagrangian onto the WET one at the EW scale μ_{EW}, with the final numerical relations summarized by Eqs. (4.1)–(4.5), which allow us to connect the values of the SMEFT Wilson coefficients given at Λ to that of the WET ones given at μ_b.

We then explored the contributions to the observables $R(D)$, $R(D^*)$, $P_\tau(D^*)$, $R(J/\psi)$, and $R(X_c)$ in the presence of a single SMEFT Wilson coefficient. It is found that the scenario with a single C_1 or C_4 can be used to resolve the $R(D^{(*)})$ anomalies at 1σ, especially with the finding that the experimental central values can be well reproduced with a single C_4. A single C_3 is, however, already ruled out by the measured $R(D^{(*)})$ and the constraint $\mathcal{B}(B_c \to \tau\nu) \lesssim 10\%$ at more than 3σ. In the case where two SMEFT Wilson coefficients are present simultaneously, on the other hand, we found that the constraints from $\Delta R(D)$ and $\Delta R(D^*)$ are the strongest, but the one from $\mathcal{B}(B_c \to \tau\nu) \lesssim 10\%$ is very complementary to them, making parts of the regions allowed by $\Delta R(D^{(*)})$ already excluded. Under the combined constraints from the measured $R(D)$, $R(D^*)$, $P_\tau(D^*)$, $R(J/\psi)$, and $R(X_c)$, we obtained the best-fit points and the allowed regions at 99.73% C.L., which are shown in Table 3 and Fig. 2, respectively. Due to the extra combined constraints from $P_\tau(D^*)$, $R(J/\psi)$, and $R(X_c)$, the scenario with a single C_4 is also found to be no better than that with a single C_1 for resolving the $R(D^{(*)})$ anomalies.

Through a global fit, we have identified eleven most trustworthy scenarios, each of which can provide a good explanation of the $R(D^{(*)})$ anomalies at 1σ. In order to further discriminate these different scenarios, we have also predicted the observables in each NP scenario and considered the correlations among them. It is found that most of the scenarios can be differentiated from each other by using these observables as well as their correlations. In particular, the predicted $\mathcal{B}(B_c \to \tau\nu)$ in the scenario S11 is found to be much smaller than in the other scenarios as well as in the SM. The observables $P_\tau(D)$, $\mathcal{X}_4(D)$, $A_{FB}(D^*)$, $P_\tau(D^*)$, $P_L(D^*)$, $\mathcal{X}_5(D^*)$, $P_\tau(\Lambda_c)$, P_{Λ_c}, $\mathcal{X}_5(\Lambda_c)$, as well as the $P_\tau(D^*) - P_L(D^*)$ and $A_{FB}(D) - P_\tau(D^*)$ correlation plots can be used to distinguish the scenario S3 from the other ones.

As both the LHCb and Belle II experiments will be in an ideal position to provide additional information by significantly reducing the uncertainties of the observables already measured and by measuring new observables that can provide complementary constraints on the NP parameters, we shall expect a better understanding of the different NP scenarios involved in $b \to c\tau\nu$ transitions.

Note added: After this work was finished, we are informed that there has been a preliminary Belle measurement of the

D^* longitudinal polarization fraction in $B \to D^* \tau \nu$ [166]. This preliminary result $P_L(D^*) = 0.60 \pm 0.08 \pm 0.035$ shall exclude the scenario S3, which predicts a very small $P_L(D^*) = 0.142 \pm 0.001$ (see Table 4). This implies that the solution to the $R(D)$ and $R(D^*)$ anomalies with the tensor operator is not favored.

Appendix: Helicity amplitudes for $\Lambda_b \to \Lambda_c \tau \nu$ decay

Here we give the explicit expressions of the helicity amplitudes for $\Lambda_b(p_{\Lambda_b}) \to \Lambda_c(p_{\Lambda_c}) \tau(p_\tau) \nu(p_\nu)$ decay calculated by ourselves. Following the helicity method described in Refs. [101–104], we can write the helicity amplitudes $\mathcal{M}_{\lambda_{\Lambda_b}}^{\lambda_{\Lambda_c}, \lambda_\tau}$ as [100]

$$\mathcal{M}_{\lambda_{\Lambda_b}}^{\lambda_{\Lambda_c}, \lambda_\tau} = H_{\lambda_{\Lambda_b}}^{(SP)\lambda_{\Lambda_c}} L^{\lambda_\tau} + \sum_\lambda \eta_\lambda H_{\lambda_{\Lambda_b}, \lambda}^{(VA)\lambda_{\Lambda_c}} L_\lambda^{\lambda_\tau}$$
$$+ \sum_{\lambda, \lambda'} \eta_\lambda \eta_{\lambda'} H_{\lambda_{\Lambda_b}, \lambda, \lambda'}^{(T)\lambda_{\Lambda_c}} L_{\lambda, \lambda'}^{\lambda_\tau}. \quad (A.1)$$

Here, H and L denote the hadronic and leptonic helicity amplitudes, respectively, $\lambda^{(\prime)}$ indicates the helicity of the virtual vector boson, with $\eta_{\lambda^{(\prime)}} = 1$ for $\lambda^{(\prime)} = t$ and $\eta_{\lambda^{(\prime)}} = -1$ for $\lambda^{(\prime)} = 0, \pm 1$, and the momentum transfer squared is given by $q^2 = (p_{\Lambda_b} - p_{\Lambda_c})^2 = (p_\tau + p_\nu)^2$.

Starting with the effective Lagrangian given by Eq. (2.9) and using the helicity-based definition of the $\Lambda_b \to \Lambda_c$ transition form factors in Refs. [100,167], we can obtain the hadronic helicity amplitudes as follows:

- The non-zero scalar and pseudo-scalar helicity amplitudes,

$$H_{-1/2}^{(SP)-1/2} = (C_{S_L} + C_{S_R}) F_0 \frac{\sqrt{Q_+}}{\overline{m}_b - \overline{m}_c} (m_{\Lambda_b} - m_{\Lambda_c})$$

$$- (C_{S_L} - C_{S_R}) G_0 \frac{\sqrt{Q_-}}{\overline{m}_b + \overline{m}_c} (m_{\Lambda_b} + m_{\Lambda_c}), \quad (A.2)$$

$$H_{1/2}^{(SP)1/2} = (C_{S_L} + C_{S_R}) F_0 \frac{\sqrt{Q_+}}{\overline{m}_b - \overline{m}_c} (m_{\Lambda_b} - m_{\Lambda_c})$$

$$+ (C_{S_L} - C_{S_R}) G_0 \frac{\sqrt{Q_-}}{\overline{m}_b + \overline{m}_c} (m_{\Lambda_b} + m_{\Lambda_c}), \quad (A.3)$$

where $\overline{m}_b$ and $\overline{m}_c$ are the b- and c-quark running masses in the $\overline{\text{MS}}$ scheme and should be evaluated at the typical energy scale μ_b.

- The non-zero vector and axial-vector helicity amplitudes,

$$H_{-1/2,0}^{(VA)-1/2} = (1 + C_{V_L} + C_{V_R}) F_+ \frac{\sqrt{Q_-}}{\sqrt{q^2}} (m_{\Lambda_b} + m_{\Lambda_c})$$

$$+ (1 + C_{V_L} - C_{V_R}) G_+ \frac{\sqrt{Q_+}}{\sqrt{q^2}} (m_{\Lambda_b} - m_{\Lambda_c}), \quad (A.4)$$

$$H_{-1/2,t}^{(VA)-1/2} = (1 + C_{V_L} + C_{V_R}) F_0 \frac{\sqrt{Q_+}}{\sqrt{q^2}} (m_{\Lambda_b} - m_{\Lambda_c})$$

$$+ (1 + C_{V_L} - C_{V_R}) G_0 \frac{\sqrt{Q_-}}{\sqrt{q^2}} (m_{\Lambda_b} + m_{\Lambda_c}), \quad (A.5)$$

$$H_{1/2,1}^{(VA)-1/2} = (1 + C_{V_L} + C_{V_R}) F_\perp \sqrt{2Q_-}$$

$$+ (1 + C_{V_L} - C_{V_R}) G_\perp \sqrt{2Q_+}, \quad (A.6)$$

$$H_{-1/2,-1}^{(VA)1/2} = (1 + C_{V_L} + C_{V_R}) F_\perp \sqrt{2Q_-}$$

$$- (1 + C_{V_L} - C_{V_R}) G_\perp \sqrt{2Q_+}, \quad (A.7)$$

$$H_{1/2,0}^{(VA)1/2} = (1 + C_{V_L} + C_{V_R}) F_+ \frac{\sqrt{Q_-}}{\sqrt{q^2}} (m_{\Lambda_b} + m_{\Lambda_c})$$

$$- (1 + C_{V_L} - C_{V_R}) G_+ \frac{\sqrt{Q_+}}{\sqrt{q^2}} (m_{\Lambda_b} - m_{\Lambda_c}), \quad (A.8)$$

$$H_{1/2,t}^{(VA)1/2} = (1 + C_{V_L} + C_{V_R}) F_0 \frac{\sqrt{Q_+}}{\sqrt{q^2}} (m_{\Lambda_b} - m_{\Lambda_c})$$

$$- (1 + C_{V_L} - C_{V_R}) G_0 \frac{\sqrt{Q_-}}{\sqrt{q^2}} (m_{\Lambda_b} + m_{\Lambda_c}). \quad (A.9)$$

- The non-zero tensor helicity amplitudes,

$$H_{-1/2,t,0}^{(T)-1/2} = H_{-1/2,1,-1}^{(T)-1/2} = C_T (h_+ \sqrt{Q_-} - \widetilde{h}_+ \sqrt{Q_+}), \quad (A.10)$$

$$H_{1/2,1,0}^{(T)-1/2} = H_{1/2,t,1}^{(T)-1/2}$$

$$= \sqrt{2} C_T \Big[h_\perp \frac{\sqrt{Q_-}}{\sqrt{q^2}} (m_{\Lambda_b} + m_{\Lambda_c})$$

$$- \widetilde{h}_\perp \frac{\sqrt{Q_+}}{\sqrt{q^2}} (m_{\Lambda_b} - m_{\Lambda_c}) \Big], \quad (A.11)$$

$$H_{-1/2,0,-1}^{(T)1/2} = H_{-1/2,t,-1}^{(T)1/2}$$
$$= \sqrt{2}C_T \left[h_\perp \frac{\sqrt{Q_-}}{\sqrt{q^2}} (m_{\Lambda_b} + m_{\Lambda_c}) \right.$$
$$\left. + \tilde{h}_\perp \frac{\sqrt{Q_+}}{\sqrt{q^2}} (m_{\Lambda_b} - m_{\Lambda_c}) \right], \quad (A.12)$$

$$H_{1/2,1,-1}^{(T)1/2} = H_{1/2,t,0}^{(T)1/2} = C_T (h_+ \sqrt{Q_-} + \tilde{h}_+ \sqrt{Q_+}), \quad (A.13)$$

together with the other non-vanishing tensor-type helicity amplitudes related to the above ones by

$$H_{\lambda_{\Lambda_b},\lambda,\lambda'}^{(T)\lambda_{\Lambda_c}} = -H_{\lambda_{\Lambda_b},\lambda',\lambda}^{(T)\lambda_{\Lambda_c}}. \quad (A.14)$$

For the leptonic helicity amplitudes, on the other hand, we obtain [100,168]:

- The non-zero scalar and pseudoscalar leptonic helicity amplitudes,

$$L^{1/2} = 2\sqrt{q^2}\, v. \quad (A.15)$$

- The non-zero vector and axial-vector amplitudes,

$$L_0^{-1/2} = 2\sqrt{q^2}\, v\, \sin(\theta_\tau), \quad (A.16)$$

$$L_{\pm 1}^{-1/2} = -\sqrt{2q^2}\, v\, [1 \mp \cos(\theta_\tau)], \quad (A.17)$$

$$L_0^{1/2} = -2\, m_\tau\, v\, \cos(\theta_\tau), \quad (A.18)$$

$$L_{\pm 1}^{1/2} = \pm\sqrt{2}\, m_\tau\, v\, \sin(\theta_\tau), \quad (A.19)$$

$$L_t^{1/2} = 2\, m_\tau\, v. \quad (A.20)$$

- The non-zero tensor amplitudes,

$$L_{0,\pm 1}^{-1/2} = \mp\sqrt{2}\, m_\tau\, v\, [1 \mp \cos(\theta_\tau)], \quad (A.21)$$

$$L_{0,t}^{-1/2} = L_{1,-1}^{-1/2} = -2\, m_\tau\, v\, \sin(\theta_\tau), \quad (A.22)$$

$$L_{\pm 1,t}^{-1/2} = \sqrt{2}\, m_\tau\, v\, [1 \mp \cos(\theta_\tau)], \quad (A.23)$$

$$L_{0,\pm 1}^{1/2} = \sqrt{2q^2}\, v\, \sin(\theta_\tau), \quad (A.24)$$

$$L_{0,t}^{1/2} = L_{1,-1}^{1/2} = 2\sqrt{q^2}\, v\, \cos(\theta_\tau), \quad (A.25)$$

$$L_{\pm 1,t}^{1/2} = \mp\sqrt{2q^2}\, v\, \sin(\theta_\tau), \quad (A.26)$$

as well as the other non-vanishing tensor-type helicity amplitudes related to the above ones by

$$L_{\lambda,\lambda'}^{\lambda_\tau} = -L_{\lambda',\lambda}^{\lambda_\tau}. \quad (A.27)$$

Integrating the twofold angular distribution given by Eq. (3.9) over $\cos\theta_\tau$ but without the first two summations over λ_{Λ_c} and λ_τ, we can obtain the following expression for the helicity-dependent differential decay rate:

$$\frac{d\Gamma^{\lambda_{\Lambda_c},\lambda_\tau}}{dq^2}$$
$$= \frac{G_F^2 |V_{cb}|^2}{2} \frac{v^2 |\mathbf{p}_{\Lambda_c}|}{256\pi^3 m_{\Lambda_b}^2} \frac{1}{2} \sum_{\lambda_{\Lambda_b}} \int_{-1}^{1} d\cos\theta_\tau |\mathcal{M}_{\lambda_{\Lambda_b}}^{\lambda_{\Lambda_c},\lambda_\tau}|^2, \quad (A.28)$$

from which we get the differential decay rates

$$\frac{d\Gamma^{\lambda_{\Lambda_c}=1/2}}{dq^2} = \sum_{\lambda_\tau} \frac{d\Gamma^{1/2,\lambda_\tau}}{dq^2},$$

$$\frac{d\Gamma^{\lambda_{\Lambda_c}=-1/2}}{dq^2} = \sum_{\lambda_\tau} \frac{d\Gamma^{-1/2,\lambda_\tau}}{dq^2}, \quad (A.29)$$

for a polarized Λ_c baryon, and

$$\frac{d\Gamma^{\lambda_\tau=1/2}}{dq^2} = \sum_{\lambda_{\Lambda_c}} \frac{d\Gamma^{\lambda_{\Lambda_c},1/2}}{dq^2},$$

$$\frac{d\Gamma^{\lambda_\tau=-1/2}}{dq^2} = \sum_{\lambda_{\Lambda_c}} \frac{d\Gamma^{\lambda_{\Lambda_c},-1/2}}{dq^2}, \quad (A.30)$$

for a polarized τ lepton.

References

1. S. Bifani, S. Descotes-Genon, A. Romero Vidal, M.-H. Schune, Review of lepton universality tests in B decays. arXiv:1809.06229
2. Y. Li, C.-D. Lü, Recent anomalies in B physics. Sci. Bull. **63**, 267–269 (2018). arXiv:1808.02990
3. G. Ciezarek, M. Franco Sevilla, B. Hamilton, R. Kowalewski, T. Kuhr, V. Lüth, Y. Sato, A challenge to lepton universality in B meson decays. Nature **546**, 227–233 (2017). arXiv:1703.01766
4. **BaBar** Collaboration, J. P. Lees et al., Evidence for an excess of $\bar{B} \to D^{(*)}\tau^-\bar{\nu}_\tau$ decays. Phys. Rev. Lett. **109**, 101802 (2012). arXiv:1205.5442
5. **BaBar** Collaboration, J. P. Lees et al., Measurement of an excess of $\bar{B} \to D^{(*)}\tau^-\bar{\nu}_\tau$ decays and implications for charged Higgs bosons. Phys. Rev. D **88**(7), 072012 (2013). arXiv:1303.0571
6. **Belle** Collaboration, M. Huschle et al., Measurement of the branching ratio of $\bar{B} \to D^{(*)}\tau^-\bar{\nu}_\tau$ relative to $\bar{B} \to D^{(*)}\ell^-\bar{\nu}_\ell$ decays with hadronic tagging at Belle. Phys. Rev. D **92**(7), 072014 (2015). arXiv:1507.03233
7. **Belle** Collaboration, Y. Sato et al., Measurement of the branching ratio of $\bar{B}^0 \to D^{*+}\tau^-\bar{\nu}_\tau$ relative to $\bar{B}^0 \to D^{*+}\ell^-\bar{\nu}_\ell$ decays with a semileptonic tagging method. Phys. Rev. D **94**(7), 072007 (2016). arXiv:1607.07923
8. **Belle** Collaboration, S. Hirose et al., Measurement of the τ lepton polarization and R(D*) in the decay $\bar{B} \to D^*\tau^-\bar{\nu}_\tau$. Phys. Rev. Lett. **118**(21), 211801 (2017). arXiv:1612.00529
9. **Belle** Collaboration, S. Hirose et al., Measurement of the τ lepton polarization and R(D*) in the decay $\bar{B} \to D^*\tau^-\bar{\nu}_\tau$ with one-prong hadronic τ decays at Belle. Phys. Rev. D**97**(1), 012004 (2018). arXiv:1709.00129

10. **LHCb** Collaboration, R. Aaij et al., Measurement of the ratio of branching fractions $\mathcal{B}(\bar{B}^0 \to D^{*+}\tau^-\bar{\nu}_\tau)/\mathcal{B}(\bar{B}^0 \to D^{*+}\mu^-\bar{\nu}_\mu)$. Phys. Rev. Lett. **115**(11), 111803 (2015). arXiv:1506.08614 (erratum: Phys. Rev. Lett. 115(15), 159901, 2015)

11. **LHCb** Collaboration, R. Aaij et al., Measurement of the ratio of the $B^0 \to D^{*-}\tau^+\nu_\tau$ and $B^0 \to D^{*-}\mu^+\nu_\mu$ branching fractions using three-prong τ-lepton decays. Phys. Rev. Lett. **120**(17), 171802 (2018). arXiv:1708.08856

12. **LHCb** Collaboration, R. Aaij et al., Test of lepton flavor universality by the measurement of the $B^0 \to D^{*-}\tau^+\nu_\tau$ branching fraction using three-prong τ decays. Phys. Rev. D **97**(7), 072013 (2018). arXiv:1711.02505

13. **HFLAV** Collaboration, Y. Amhis et al., Averages of b-hadron, c-hadron, and τ-lepton properties as of summer 2016. Eur. Phys. J. C **77**(12), 895 (2017). arXiv:1612.07233

14. **HFLAV** Collaboration, Online update for averages of R_D and R_{D^*} for summer 2018. https://hflav-eos.web.cern.ch/hflav-eos/semi/summer18/RDRDs.html

15. D. Bigi, P. Gambino, Revisiting $B \to D\ell\nu$. Phys. Rev. D **94**(9), 094008 (2016). arXiv:1606.08030

16. F.U. Bernlochner, Z. Ligeti, M. Papucci, D.J. Robinson, Combined analysis of semileptonic B decays to D and D^*: $R(D^{(*)})$, $|V_{cb}|$, and new physics. Phys. Rev. D **95**(11), 115008 (2017). arXiv:1703.05330 (erratum Phys. Rev. D 97(5), 059902, 2018)

17. D. Bigi, P. Gambino, S. Schacht, $R(D^*)$, $|V_{cb}|$, and the heavy quark symmetry relations between form factors. JHEP **11**, 061 (2017). arXiv:1707.09509

18. S. Jaiswal, S. Nandi, S.K. Patra, Extraction of $|V_{cb}|$ from $B \to D^{(*)}\ell\nu_\ell$ and the Standard Model predictions of $R(D^{(*)})$. JHEP **12**, 060 (2017). arXiv:1707.09977

19. Q.-Y. Hu, X.-Q. Li, Y. Muramatsu, Y.-D. Yang, R-parity violating solutions to the $R_{D^{(*)}}$ anomaly and their GUT-scale unifications. arXiv:1808.01419

20. M. Carena, E. Megías, M. Quirós, C. Wagner, $R_{D^{(*)}}$ in custodial warped space. arXiv:1809.01107

21. T.D. Cohen, H. Lamm, R.F. Lebed, Tests of the standard model in $B \to D\ell\nu_\ell$, $B \to D^*\ell\nu_\ell$ and $B_c \to J/\psi\ell\nu_\ell$. Phys. Rev. D **98**(3), 034022 (2018). arXiv:1807.00256

22. J. Heeck, D. Teresi, Pati–Salam explanations of the B-meson anomalies. arXiv:1808.07492

23. A. Angelescu, D. Bečirević, D.A. Faroughy, O. Sumensari, Closing the window on single leptoquark solutions to the B-physics anomalies. arXiv:1808.08179

24. Z.-R. Huang, Y. Li, C.-D. Lu, M.A. Paracha, C. Wang, Footprints of new physics in $b \to c\tau\nu$ transitions. arXiv:1808.03565

25. A. Azatov, D. Barducci, D. Ghosh, D. Marzocca, L. Ubaldi, Combined explanations of B-physics anomalies: the sterile neutrino solution. arXiv:1807.10745

26. S.-P. Li, X.-Q. Li, Y.-D. Yang, X. Zhang, $R_{D^{(*)}}$, $R_{K^{(*)}}$ and neutrino mass in the 2HDM-III with right-handed neutrinos. arXiv:1807.08530

27. D. Robinson, B. Shakya, J. Zupan, Right-handed neutrinos and $R(D^{(*)})$. arXiv:1807.04753

28. S. Trifinopoulos, Revisiting R-parity violating interactions as an explanation of the B-physics anomalies. Eur. Phys. J. C **78**(10), 803 (2018). arXiv:1807.01638

29. F. Feruglio, P. Paradisi, O. Sumensari, Implications of scalar and tensor explanations of $R_{D^{(*)}}$. arXiv:1806.10155

30. J. Kumar, D. London, R. Watanabe, Combined explanations of the $b \to s\mu^+\mu^-$ and $b \to c\tau^-\bar{\nu}$ anomalies: a general model analysis. arXiv:1806.07403

31. D. Bečirević, I. Doršner, S. Fajfer, D.A. Faroughy, N. Košnik, O. Sumensari, Scalar leptoquarks from grand unified theories to accommodate the B-physics anomalies. Phys. Rev. D **98**(5), 055003 (2018). arXiv:1806.05689

32. L. Dhargyal, S.K. Rai, Implications of a vector-like lepton doublet and scalar leptoquark on $R(D^{(*)})$. arXiv:1806.01178

33. S. Bhattacharya, S. Nandi, S. Kumar Patra, $b \to c\tau\nu_\tau$ decays: a catalogue to compare, constrain, and correlate new physics effects. arXiv:1805.08222

34. S. Fraser, C. Marzo, L. Marzola, M. Raidal, C. Spethmann, Towards a viable scalar interpretation of $R_{D^{(*)}}$. Phys. Rev. D **98**(3), 035016 (2018). arXiv:1805.08189

35. R. Martinez, C.F. Sierra, G. Valencia, Beyond $\mathcal{R}(D^{(*)})$ with the general 2HDM-III for $b \to c\tau\nu$. arXiv:1805.04098

36. A. Azatov, D. Bardhan, D. Ghosh, F. Sgarlata, E. Venturini, Anatomy of $b \to c\tau\nu$ anomalies. arXiv:1805.03209

37. A.K. Alok, D. Kumar, S. Kumbhakar, S. Uma Sankar, Resolution of R_D/R_{D^*} puzzle. Phys. Lett **B784**, 16–20 (2018). arXiv:1804.08078

38. U. Aydemir, D. Minic, C. Sun, T. Takeuchi, B-decay anomalies and scalar leptoquarks in unified Pati–Salam models from non-commutative geometry. JHEP **09**, 117 (2018). arXiv:1804.05844

39. A. Greljo, D.J. Robinson, B. Shakya, J. Zupan, $R(D^{(*)})$ from W' and right-handed neutrinos. JHEP **09**, 169 (2018). arXiv:1804.04642

40. P. Asadi, M.R. Buckley, D. Shih, It's all right(-handed neutrinos): a new W' model for the $R_{D^{(*)}}$ anomaly. JHEP **09**, 010 (2018). arXiv:1804.04135

41. D. Marzocca, Addressing the B-physics anomalies in a fundamental composite Higgs model. JHEP **07**, 121 (2018). arXiv:1803.10972

42. Z.-J. Yang, S.-M. Zhao, X.-X. Dong, X.-J. Zhan, H.-B. Zhang, T.-F. Feng, The corrections to R_D and R_{D^*} in BLMSSM. arXiv:1802.01769

43. S. Iguro, Y. Omura, Status of the semileptonic B decays and muon $g - 2$ in general 2HDMs with right-handed neutrinos. JHEP **05**, 173 (2018). arXiv:1802.01732

44. P. Colangelo, F. De Fazio, Scrutinizing $\bar{B} \to D^* (D\pi)\ell^-\bar{\nu}_\ell$ and $\bar{B} \to D^* (D\gamma)\ell^-\bar{\nu}_\ell$ in search of new physics footprints. JHEP **06**, 082 (2018). arXiv:1801.10468

45. A. Biswas, D.K. Ghosh, A. Shaw, S.K. Patra, $b \to c\ell\nu$ anomalies in light of extended scalar sectors. arXiv:1801.03375

46. M. Jung, D.M. Straub, Constraining new physics in $b \to c\ell\nu$ transitions. arXiv:1801.01112

47. D. Choudhury, A. Kundu, R. Mandal, R. Sinha, $R_{K^{(*)}}$ and $R(D^{(*)})$ anomalies resolved with lepton mixing. Nucl. Phys. B **933**, 433–453 (2018). arXiv:1712.01593

48. X.-G. He, G. Valencia, Lepton universality violation and right-handed currents in $b \to c\tau\nu$. Phys. Lett. B **779**, 52–57 (2018). arXiv:1711.09525

49. D. Bardhan, P. Byakti, D. Ghosh, A closer look at the R_D and R_{D^*} anomalies. JHEP **01**, 125 (2017). arXiv:1610.03038

50. A. Crivellin, J. Heeck, P. Stoffer, A perturbed lepton-specific two-Higgs-doublet model facing experimental hints for physics beyond the Standard Model. Phys. Rev. Lett. **116**(8), 081801 (2016). arXiv:1507.07567

51. S. Fajfer, J.F. Kamenik, I. Nisandzic, On the $B \to D^*\tau\bar{\nu}_\tau$ sensitivity to new physics. Phys. Rev. D **85**, 094025 (2012). arXiv:1203.2654

52. S. Fajfer, J.F. Kamenik, I. Nisandzic, J. Zupan, Implications of lepton flavor universality violations in B decays. Phys. Rev. Lett. **109**, 161801 (2012). arXiv:1206.1872

53. A. Crivellin, C. Greub, A. Kokulu, Explaining $B \to D\tau\nu$, $B \to D^*\tau\nu$ and $B \to \tau\nu$ in a 2HDM of type III. Phys. Rev. D **86**, 054014 (2012). arXiv:1206.2634

54. A.K. Alok, D. Kumar, J. Kumar, S. Kumbhakar, S.U. Sankar, New physics solutions for R_D and R_{D^*}. JHEP **09**, 152 (2018). arXiv:1710.04127

55. W. Buchmuller, D. Wyler, Effective Lagrangian analysis of new interactions and flavor conservation. Nucl. Phys. B **268**, 621–653 (1986)

56. B. Grzadkowski, M. Iskrzynski, M. Misiak, J. Rosiek, Dimension-six terms in the Standard Model Lagrangian. JHEP **10**, 085 (2010). arXiv:1008.4884

57. S. Weinberg, Effective gauge theories. Phys. Lett. **91B**, 51–55 (1980)

58. S.R. Coleman, J. Wess, B. Zumino, Structure of phenomenological Lagrangians. 1. Phys. Rev. **177**, 2239–2247 (1969)

59. C.G. Callan Jr., S.R. Coleman, J. Wess, B. Zumino, Structure of phenomenological Lagrangians. 2. Phys. Rev. **177**, 2247–2250 (1969)

60. S. Willenbrock, C. Zhang, Effective field theory beyond the Standard Model. Ann. Rev. Nucl. Part. Sci. **64**, 83–100 (2014). arXiv:1401.0470

61. A. Falkowski, Effective field theory approach to LHC Higgs data. Pramana **87**(3), 39 (2016). arXiv:1505.00046

62. I. Brivio , M. Trott, The Standard Model as an effective field theory. arXiv:1706.08945

63. **LHC Higgs Cross Section Working Group** Collaboration, D. de Florian et al., Handbook of LHC Higgs Cross Sections: 4. Deciphering the Nature of the Higgs Sector. arXiv:1610.07922

64. S. Weinberg, Baryon and lepton nonconserving processes. Phys. Rev. Lett. **43**, 1566–1570 (1979)

65. K. Hagiwara, S. Ishihara, R. Szalapski, D. Zeppenfeld, Low-energy effects of new interactions in the electroweak boson sector. Phys. Rev. D **48**, 2182–2203 (1993)

66. R. Contino, M. Ghezzi, C. Grojean, M. Muhlleitner, M. Spira, Effective Lagrangian for a light Higgs-like scalar. JHEP **07**, 035 (2013). arXiv:1303.3876

67. G.F. Giudice, C. Grojean, A. Pomarol, R. Rattazzi, The strongly-interacting light Higgs. JHEP **06**, 045 (2007). arXiv:hep-ph/0703164

68. A. Falkowski, B. Fuks, K. Mawatari, K. Mimasu, F. Riva, V. Sanz, Rosetta: an operator basis translator for Standard Model effective field theory. Eur. Phys. J. C **75**(12), 583 (2015). arXiv:1508.05895

69. J. Aebischer et al., WCxf: an exchange format for Wilson coefficients beyond the Standard Model. Comput. Phys. Commun. **232**, 71–83 (2018). arXiv:1712.05298

70. E.E. Jenkins, A.V. Manohar, M. Trott, Renormalization group evolution of the Standard Model dimension six operators I: formalism and lambda dependence. JHEP **10**, 087 (2013). arXiv:1308.2627

71. E.E. Jenkins, A.V. Manohar, M. Trott, Renormalization group evolution of the Standard Model dimension six operators II: Yukawa dependence. JHEP **01**, 035 (2014). arXiv:1310.4838

72. R. Alonso, E.E. Jenkins, A.V. Manohar, M. Trott, Renormalization group evolution of the Standard Model dimension six operators III: gauge coupling dependence and phenomenology. JHEP **04**, 159 (2014). arXiv:1312.2014

73. G. Buchalla, A.J. Buras, M.E. Lautenbacher, Weak decays beyond leading logarithms. Rev. Mod. Phys. **68**, 1125–1144 (1996). arXiv:hep-ph/9512380

74. A.J. Buras, Weak Hamiltonian, CP violation and rare decays, in probing the standard model of particle interactions. Proceedings, Summer School in Theoretical Physics, NATO Advanced Study Institute, 68th session, Les Houches, July 28–September 5, 1997. Pt. 1, 2, pp. 281–539 (1998). arXiv:hep-ph/9806471

75. J. Aebischer, M. Fael, C. Greub, J. Virto, B physics beyond the Standard Model at one loop: complete renormalization group evolution below the electroweak scale. JHEP **09**, 158 (2017). arXiv:1704.06639

76. E.E. Jenkins, A.V. Manohar, P. Stoffer, Low-energy effective field theory below the electroweak scale: operators and matching. JHEP **03**, 016 (2018). arXiv:1709.04486

77. E.E. Jenkins, A.V. Manohar, P. Stoffer, Low-energy effective field theory below the electroweak scale: anomalous dimensions. JHEP **01**, 084 (2018). arXiv:1711.05270

78. J. Aebischer, J. Kumar, D.M. Straub, Wilson: a Python package for the running and matching of Wilson coefficients above and below the electroweak scale. arXiv:1804.05033

79. J. Aebischer, A. Crivellin, M. Fael, C. Greub, Matching of gauge invariant dimension-six operators for $b \to s$ and $b \to c$ transitions. JHEP **05**, 037 (2016). arXiv:1512.02830

80. F. Feruglio, P. Paradisi, A. Pattori, Revisiting lepton flavor universality in B decays. Phys. Rev. Lett. **118**(1), 011801 (2017). arXiv:1606.00524

81. F. Feruglio, P. Paradisi, A. Pattori, On the importance of electroweak corrections for B anomalies. JHEP **09**, 061 (2017). arXiv:1705.00929

82. M. González-Alonso, J. Martin Camalich, K. Mimouni, Renormalization-group evolution of new physics contributions to (semi)leptonic meson decays. Phys. Lett **B772**, 777–785 (2017). arXiv:1706.00410

83. R. Alonso, E.E. Jenkins, A.V. Manohar, M. Trott, Dimension-Six Renormalization Group Equations. http://einstein.ucsd.edu/smeft/

84. A. Dedes, W. Materkowska, M. Paraskevas, J. Rosiek, K. Suxho, Feynman rules for the Standard Model effective field theory in R_ξ-gauges. JHEP **06**, 143 (2017). arXiv:1704.03888

85. R. Alonso, B. Grinstein, J. Martin Camalich, Lepton universality violation and lepton flavor conservation in B-meson decays. JHEP **10**, 184 (2015). arXiv:1505.05164

86. O. Catá, M. Jung, Signatures of a nonstandard Higgs boson from flavor physics. Phys. Rev. D **92**(5), 055018 (2015). arXiv:1505.05804

87. V. Cirigliano, J. Jenkins, M. Gonzalez-Alonso, Semileptonic decays of light quarks beyond the Standard Model. Nucl. Phys. B **830**, 95–115 (2010). arXiv:0908.1754

88. B. Capdevila, A. Crivellin, S. Descotes-Genon, L. Hofer, J. Matias, Searching for new physics with $b \to s\tau^+\tau^-$ processes. Phys. Rev. Lett. **120**(18), 181802 (2018). arXiv:1712.01919

89. A. Sirlin, Large m_W, m_Z behavior of the $O(\alpha)$ corrections to semileptonic processes mediated by W. Nucl. Phys. B **196**, 83–92 (1982)

90. W.J. Marciano, A. Sirlin, Radiative corrections to π_{l2} decays. Phys. Rev. Lett. **71**, 3629–3632 (1993)

91. M.B. Voloshin, Upper bound on tensor interaction in the decay $\pi^- \to e^- \nu\gamma$. Phys. Lett. B **283**, 120–122 (1992)

92. E. Eichten, B.R. Hill, An effective field theory for the calculation of matrix elements involving heavy quarks. Phys. Lett. B **234**, 511–516 (1990)

93. J.A. Gracey, Three loop $\overline{MS}$ tensor current anomalous dimension in QCD. Phys. Lett. B **488**, 175–181 (2000). arXiv:hep-ph/0007171

94. A. Celis, J. Fuentes-Martin, A. Vicente, J. Virto, DsixTools: the Standard Model effective field theory toolkit. Eur. Phys. J. C **77**(6), 405 (2017). arXiv:1704.04504

95. A. Celis, M. Jung, X.-Q. Li, A. Pich, Sensitivity to charged scalars in $B \to D^{(*)}\tau\nu_\tau$ and $B \to \tau\nu_\tau$ decays. JHEP **01**, 054 (2013). arXiv:1210.8443

96. A. Datta, M. Duraisamy, D. Ghosh, Diagnosing new physics in $b \to c \tau \nu_\tau$ decays in the light of the recent BaBar result. Phys. Rev. D **86**, 034027 (2012). arXiv:1206.3760

97. Y. Sakaki, M. Tanaka, A. Tayduganov, R. Watanabe, Testing leptoquark models in $\bar{B} \to D^{(*)}\tau\bar{\nu}$. Phys. Rev. D **88**(9), 094012 (2013). arXiv:1309.0301

98. T. Gutsche, M. A. Ivanov, J. G. Körner, V. E. Lyubovitskij, P. Santorelli, N. Habyl, Semileptonic decay $\Lambda_b \to \Lambda_c + \tau^- + \bar{\nu_\tau}$ in the covariant confined quark model. Phys. Rev. D **91**(7),

074001 (2015). arXiv:1502.04864 (erratum: Phys. Rev. D 91(11), 119907, 2015)

99. X.-Q. Li, Y.-D. Yang, X. Zhang, $\Lambda_b \rightarrow \Lambda_c \tau \bar{\nu}_\tau$ decay in scalar and vector leptoquark scenarios. JHEP **02**, 068 (2017). arXiv:1611.01635

100. A. Datta, S. Kamali, S. Meinel, A. Rashed, Phenomenology of $\Lambda_b \rightarrow \Lambda_c \tau \bar{\nu}_\tau$ using lattice QCD calculations. JHEP **08**, 131 (2017). arXiv:1702.02243

101. J.G. Korner, G.A. Schuler, Exclusive semileptonic decays of bottom mesons in the spectator quark model. Z. Phys. C **38**, 511 (1988) (erratum: Z. Phys. C 41, 690, 1989)

102. J.G. Korner, G.A. Schuler, Lepton mass effects in semileptonic B meson decays. Phys. Lett. B **231**, 306–311 (1989)

103. J.G. Korner, G.A. Schuler, Exclusive semileptonic heavy meson decays including lepton mass effects. Z. Phys. C **46**, 93 (1990)

104. J. Gratrex, M. Hopfer, R. Zwicky, Generalised helicity formalism, higher moments and the $B \rightarrow K_{J_K}(\rightarrow K\pi)\bar{\ell}_1\ell_2$ angular distributions. Phys. Rev. D **93**(5), 054008 (2016). arXiv:1506.03970

105. W. Detmold, C. Lehner, S. Meinel, $\Lambda_b \rightarrow p\ell^-\bar{\nu}_\ell$ and $\Lambda_b \rightarrow \Lambda_c\ell^-\bar{\nu}_\ell$ form factors from lattice QCD with relativistic heavy quarks. Phys. Rev. D **92**(3), 034503 (2015). arXiv:1503.01421

106. M.A. Ivanov, J.G. Korner, P. Santorelli, The semileptonic decays of the B_c meson. Phys. Rev. D **63**, 074010 (2001). arXiv:hep-ph/0007169

107. D. Ebert, R.N. Faustov, V.O. Galkin, Weak decays of the B_c meson to charmonium and D mesons in the relativistic quark model. Phys. Rev. D **68**, 094020 (2003). arXiv:hep-ph/0306306

108. E. Hernandez, J. Nieves, J.M. Verde-Velasco, Study of exclusive semileptonic and non-leptonic decays of B_c—in a non-relativistic quark model. Phys. Rev. D **74**, 074008 (2006). arXiv:hep-ph/0607150

109. M.A. Ivanov, J.G. Körner, P. Santorelli, Exclusive semileptonic and nonleptonic decays of the B_c meson. Phys. Rev. D **73**, 054024 (2006). arXiv:hep-ph/0602050

110. W. Wang, Y.-L. Shen, C.-D. Lu, Covariant light-front approach for B_c transition form factors. Phys. Rev. D **79**, 054012 (2009). arXiv:0811.3748

111. C.-F. Qiao, R.-L. Zhu, Estimation of semileptonic decays of B_c meson to S-wave charmonia with nonrelativistic QCD. Phys. Rev. D **87**(1), 014009 (2013). arXiv:1208.5916

112. W.-F. Wang, Y.-Y. Fan, Z.-J. Xiao, Semileptonic decays $B_c \rightarrow (\eta_c, J/\Psi)l\nu$ in the perturbative QCD approach. Chin. Phys. C **37**, 093102 (2013). arXiv:1212.5903

113. Z. Rui, H. Li, G.-X. Wang, Y. Xiao, Semileptonic decays of B_c meson to S-wave charmonium states in the perturbative QCD approach. Eur. Phys. J. C **76**(10), 564 (2016). arXiv:1602.08918

114. A. Issadykov, M.A. Ivanov, The decays $B_c \rightarrow J/\psi + \bar{\ell}\nu_\ell$ and $B_c \rightarrow J/\psi + \pi(K)$ in covariant confined quark model. Phys. Lett. B **783**, 178–182 (2018). arXiv:1804.00472

115. V.V. Kiselev, A.K. Likhoded, A.I. Onishchenko, Semileptonic B_c meson decays in sum rules of QCD and NRQCD. Nucl. Phys. B **569**, 473–504 (2000). arXiv: hep-ph/9905359

116. R. Dutta, A. Bhol, $B_c \rightarrow (J/\psi, \eta_c)\tau\nu$ semileptonic decays within the standard model and beyond. Phys. Rev. D **96**(7), 076001 (2017). arXiv:1701.08598

117. R. Watanabe, New physics effect on $B_c \rightarrow J/\psi\tau\bar{\nu}$ in relation to the $R_{D^{(*)}}$ anomaly. Phys. Lett. B **776**, 5–9 (2018). arXiv:1709.08644

118. C.-T. Tran, M.A. Ivanov, J.G. Körner, P. Santorelli, Implications of new physics in the decays $B_c \rightarrow (J/\psi, \eta_c)\tau\nu$. Phys. Rev. D **97**(5), 054014 (2018). arXiv:1801.06927

119. **LHCb** Collaboration, R. Aaij et al., Measurement of the ratio of branching fractions $\mathcal{B}(B_c^+ \rightarrow J/\psi\tau^+\nu_\tau)/\mathcal{B}(B_c^+ \rightarrow J/\psi\mu^+\nu_\mu)$. Phys. Rev. Lett. **120** (12), 121801 (2018). arXiv:1711.05623

120. T.D. Cohen, H. Lamm, R.F. Lebed, Model-independent bounds on $R(J/\psi)$. JHEP **09**, 168 (2018). arXiv:1807.02730

121. C.W. Murphy , A. Soni, Model-independent determination of $B_c^+ \rightarrow \eta_c \ell^+ \nu$ form factors. arXiv:1808.05932

122. W. Wang, R. Zhu, Model independent investigation of the $R_{J/\psi,\eta_c}$ and ratios of decay widths of semileptonic B_c decays into a P-wave charmonium. arXiv:1808.10830

123. A. Berns , H. Lamm, Model-independent prediction of $R(\eta_c)$. arXiv:1808.07360

124. **HPQCD** Collaboration, B. Colquhoun, C. Davies, J. Koponen, A. Lytle, C. McNeile, B_c decays from highly improved staggered quarks and NRQCD, PoS **LATTICE2016**, 281 (2016). arXiv:1611.01987

125. A. Lytle, B. Colquhoun, C. Davies, J. Koponen, C. McNeile, Semileptonic B_c decays from full lattice QCD. PoS **BEAUTY2016**, 069 (2016). arXiv:1605.05645

126. T. Mannel, A.V. Rusov, F. Shahriaran, Inclusive semitauonic B decays to order $\mathcal{O}(\Lambda_{QCD}^3/m_b^3)$. Nucl. Phys. B **921**, 211–224 (2017). arXiv:1702.01089

127. A.F. Falk, Z. Ligeti, M. Neubert, Y. Nir, Heavy quark expansion for the inclusive decay $\bar{B} \rightarrow \tau\bar{\nu}X$. Phys. Lett. B **326**, 145–153 (1994). arXiv:hep-ph/9401226

128. S. Balk, J.G. Korner, D. Pirjol, K. Schilcher, Inclusive semileptonic B decays in QCD including lepton mass effects. Z. Phys. C **64**, 37–44 (1994). arXiv:hep-ph/9312220

129. A. Czarnecki, M. Jezabek, J.H. Kuhn, Radiative corrections to $b \rightarrow c\tau\bar{\nu}_\tau$. Phys. Lett. B **346**, 335–341 (1995). arXiv:hep-ph/9411282

130. M. Jezabek, L. Motyka, Tau lepton distributions in semileptonic B decays. Nucl. Phys. B **501**, 207–223 (1997). arXiv:hep-ph/9701358

131. S. Biswas, K. Melnikov, Second order QCD corrections to inclusive semileptonic $b \rightarrow X_c l\bar{\nu}_l$ decays with massless and massive lepton. JHEP **02**, 089 (2010). arXiv:0911.4142

132. A. Alberti, P. Gambino, K.J. Healey, S. Nandi, Precision determination of the Cabibbo–Kobayashi–Maskawa element V_{cb}. Phys. Rev. Lett. **114**(6), 061802 (2015). arXiv:1411.6560

133. I.I.Y. Bigi, M.A. Shifman, N. Uraltsev, A.I. Vainshtein, High power n of m_b in beauty widths and $n = 5 \rightarrow \infty$ limit. Phys. Rev. D **56**, 4017–4030 (1997). arXiv:hep-ph/9704245

134. W.D. Goldberger, Semileptonic B decays as a probe of new physics. arXiv:hep-ph/9902311

135. Y. Grossman, Z. Ligeti, The inclusive $\bar{B} \rightarrow \tau\bar{\nu}X$ decay in two Higgs doublet models. Phys. Lett. B **332**, 373–380 (1994). arXiv:hep-ph/9403376

136. M. Freytsis, Z. Ligeti, J.T. Ruderman, Flavor models for $\bar{B} \rightarrow D^{(*)}\tau\bar{\nu}$. Phys. Rev. D **92**(5), 054018 (2015). arXiv:1506.08896

137. P. Colangelo, F. De Fazio, Tension in the inclusive versus exclusive determinations of $|V_{cb}|$: a possible role of new physics. Phys. Rev. D **95**(1), 011701 (2017). arXiv:1611.07387

138. X.-Q. Li, Y.-D. Yang, X. Zhang, Revisiting the one leptoquark solution to the $R(D^{(*)})$ anomalies and its phenomenological implications. JHEP **08**, 054 (2016). arXiv:1605.09308

139. A. Celis, M. Jung, X.-Q. Li, A. Pich, Scalar contributions to $b \rightarrow c(u)\tau\nu$ transitions. Phys. Lett. B **771**, 168–179 (2017). arXiv:1612.07757

140. S. Kamali, A. Rashed, A. Datta, New physics in inclusive $B \rightarrow X_c\ell\bar{\nu}$ decay in light of $R(D^{(*)})$ measurements. Phys. Rev. D **97**(9), 095034 (2018). arXiv:1801.08259

141. I.P. Gouz, V.V. Kiselev, A.K. Likhoded, V.I. Romanovsky, O.P. Yushchenko, Prospects for the B_c studies at LHCb. Phys. Atom. Nucl. **67**, 1559–1570 (2004). arXiv:hep-ph/0211432 (Yad. Fiz. 67, 1581, 2004)

142. R. Alonso, B. Grinstein, J. Martin Camalich, Lifetime of B_c^- constrains explanations for anomalies in $B \rightarrow D^{(*)}\tau\nu$. Phys. Rev. Lett **118**(8), 081802 (2017). arXiv:1611.06676

143. A.G. Akeroyd, C.-H. Chen, Constraint on the branching ratio of $B_c \to \tau\bar{\nu}$ from LEP1 and consequences for $R(D^{(*)})$ anomaly. Phys. Rev. D **96**(7), 075011 (2017). arXiv:1708.04072

144. **HPQCD** Collaboration, B. Colquhoun, C.T.H. Davies, R.J. Dowdall, J. Kettle, J. Koponen, G.P. Lepage, A.T. Lytle, B-meson decay constants: a more complete picture from full lattice QCD. Phys. Rev. D **91**(11), 114509 (2015). arXiv:1503.05762

145. S. Descotes-Genon, P. Koppenburg, The CKM parameters. Ann. Rev. Nucl. Part. Sci. **67**, 97–127 (2017). arXiv:1702.08834

146. M. Tanabashi et al., Review of particle physics. Phys. Rev. D **98**(3), 030001 (2018)

147. **CDF, DELPHI, ALEPH, SLD, OPAL, L3** Collaboration, D. Abbaneo et al., Combined results on b hadron production rates and decay properties. arXiv: hep-ex/0112028

148. **Belle II** Collaboration, E. Kou et al., The Belle II Physics Book. arXiv:1808.10567

149. M. González-Alonso, J. Martin Camalich, Global effective-field-theory analysis of new-physics effects in (semi)leptonic kaon decays. JHEP **12**, 052 (2016). arXiv:1605.07114

150. **Belle** Collaboration, O. Lutz et al., Search for $B \to h^{(*)}\nu\bar{\nu}$ with the full Belle $\Upsilon(4S)$ data sample. Phys. Rev. D **87** (11), 111103 (2013). arXiv:1303.3719

151. **BaBar** Collaboration, J.P. Lees et al., Search for $B \to K^{(*)}\nu\bar{\nu}$ and invisible quarkonium decays. Phys. Rev. D **87**(11), 112005 (2013). arXiv:1303.7465

152. W. Altmannshofer, A.J. Buras, D.M. Straub, M. Wick, New strategies for new physics search in $B \to K^*\nu\bar{\nu}$, $B \to K\nu\bar{\nu}$ and $B \to X_s\nu\bar{\nu}$ decays. JHEP **04**, 022 (2009). arXiv:0902.0160

153. M. Bartsch, M. Beylich, G. Buchalla, D.N. Gao, Precision flavour physics with $B \to K\nu\bar{\nu}$ and $B \to Kl^+l^-$. JHEP **11**, 011 (2009). arXiv:0909.1512

154. A.J. Buras, J. Girrbach-Noe, C. Niehoff, D.M. Straub, $B \to K^{(*)}\nu\bar{\nu}$ decays in the Standard Model and beyond. JHEP **02**, 184 (2015). arXiv:1409.4557

155. D. Bečirević, S. Fajfer, N. Košnik, Lepton flavor nonuniversality in $b \to s\ell^+\ell^-$ processes. Phys. Rev. **D92**(1), 014016 (2015). arXiv:1503.09024

156. A. Celis, J. Fuentes-Martin, M. Jung, H. Serodio, Family nonuniversal $Z\prime$ models with protected flavor-changing interactions. Phys. Rev. D **92**(1), 015007 (2015). arXiv:1505.03079

157. L. Calibbi, A. Crivellin, T. Ota, Effective field theory approach to $b \to s\ell\ell^{(\prime)}$, $B \to K^{(*)}\nu\bar{\nu}$ and $B \to D^{(*)}\tau\nu$ with third generation couplings. Phys. Rev. Lett. **115**, 181801 (2015). arXiv:1506.02661

158. M. Bauer, M. Neubert, Minimal leptoquark explanation for the $R_{D^{(*)}}$, R_K, and $(g-2)_\mu$ anomalies. Phys. Rev. Lett. **116**(14), 141802 (2016). arXiv:1511.01900

159. S. Fajfer, N. Košnik, Vector leptoquark resolution of R_K and $R_{D^{(*)}}$ puzzles. Phys. Lett. B **755**, 270–274 (2016). arXiv:1511.06024

160. R. Barbieri, G. Isidori, A. Pattori, F. Senia, Anomalies in B-decays and $U(2)$ flavour symmetry. Eur. Phys. J. C **76**(2), 67 (2016). arXiv:1512.01560

161. N.G. Deshpande, X.-G. He, Consequences of R-parity violating interactions for anomalies in $\bar{B} \to D^{(*)}\tau\bar{\nu}$ and $b \to s\mu^+\mu^-$. Eur. Phys. J. C **77**(2), 134 (2017). arXiv:1608.04817

162. W. Altmannshofer, P. Bhupal Dev, A. Soni, $R_{D^{(*)}}$ anomaly: a possible hint for natural supersymmetry with R-parity violation. Phys. Rev. **D96**(9), 095010 (2017). arXiv:1704.06659

163. **ATLAS** Collaboration, G. Aad et al., A search for high-mass resonances decaying to $\tau^+\tau^-$ in pp collisions at $\sqrt{s} = 8$ TeV with the ATLAS detector. JHEP **07** , 157 (2015). arXiv:1502.07177

164. **ATLAS** Collaboration, M. Aaboud et al., Search for minimal supersymmetric Standard Model Higgs bosons H/A and for a Z' boson in the $\tau\tau$ final state produced in pp collisions at $\sqrt{s} = 13$ TeV with the ATLAS Detector. Eur. Phys. J. C **76** (11) , 585 (2016). arXiv:1608.00890

165. D.A. Faroughy, A. Greljo, J.F. Kamenik, Confronting lepton flavor universality violation in B decays with high-p_T tau lepton searches at LHC. Phys. Lett. B **764**, 126–134 (2017). arXiv:1609.07138

166. K. Adamczyk, B to semitauonic decays at Belle/Belle II, talk given at CKM2018

167. T. Feldmann, M.W.Y. Yip, Form factors for $\Lambda_b \to \Lambda$ transitions in SCET. Phys. Rev. D **85**, 014035 (2012). arXiv:1111.1844 (erratum: Phys. Rev. D 86, 079901, 2012)

168. M. Tanaka, R. Watanabe, New physics in the weak interaction of $\bar{B} \to D^{(*)}\tau\bar{\nu}$. Phys. Rev. D **87**(3), 034028 (2013). arXiv:1212.1878